

Approximate State Space Modelling of Unobserved Fractional Components

Tobias Hartl^{1,2} and Roland Weigand^{*3}

¹University of Regensburg, 93053 Regensburg, Germany

²Institute for Employment Research (IAB), 90478 Nuremberg, Germany

³AOK Bayern, 93055 Regensburg, Germany

March 2020

Abstract. We propose convenient inferential methods for potentially nonstationary multivariate unobserved components models with fractional integration and cointegration. Based on finite-order ARMA approximations in the state space representation, maximum likelihood estimation can make use of the EM algorithm and related techniques. The approximation outperforms the frequently used autoregressive or moving average truncation, both in terms of computational costs and with respect to approximation quality. Monte Carlo simulations reveal good estimation properties of the proposed methods for processes of different complexity and dimension.

Keywords. Long memory, fractional cointegration, state space, unobserved components.

JEL-Classification. C32, C51, C53, C58.

*Corresponding author. E-Mail: roland.weigand@posteo.de

1 Introduction

Fractionally integrated time series models have gained significant interest in recent decades. In possibly nonstationary multivariate setups, which arguably bear most potential e.g. for assessing macroeconomic linkages, and which are essential for the joint modelling of financial processes, several parametric models have been explored. Among the most popular are the fractionally integrated VAR model (Nielsen; 2004), the triangular fractional cointegration model of Robinson and Hualde (2003) and the cointegrated $\text{VAR}_{d,b}$ model of Johansen (2008).

Meanwhile, also models with unobserved fractional components have proven useful, as empirical and methodological work by Ray and Tsay (2000), Morana (2004), Chen and Hurvich (2006), Morana (2007) and Luciani and Veredas (2015) documents. The unobserved fractional components model allows for a generalization of the classic trend-cycle decomposition, where the long-run component is typically assumed to be $I(1)$. As Hartl et al. (2020) show, the model can be used to test the $I(1)$ assumption against a fractional alternative. Furthermore, unobserved fractional components allow the formulation of parsimonious models, like factor models, in an interpretable way.

These methods offer a variety of potential applications to empirical researchers. Long-run components of GDP, (un-)employment, and inflation are typically estimated via unobserved components models that restrict the integration order to unity (cf. e.g. Morley et al.; 2003; Doménech and Gómez; 2006; Klinger and Weber; 2016). Since there is comprehensive evidence for long memory in these variables (see e.g. Hassler and Wolters; 1995; van Dijk et al.; 2002; Tschernig et al.; 2013) unobserved fractional components may provide new insights regarding the form and persistence of the long-run components. On the other hand, fractionally integrated factor models are constructed straightforwardly using fractional unobserved components. They can be used to assess fractional cointegration relations and for forecasting, as Hartl and Weigand (2019) demonstrate.

Inferential methods for such unobserved fractional components are the subject of this paper. So far, the bulk of empirical work in this field has been conducted in a semiparametric setting, which may be explained by the high computational and implementation cost of state-of-the-art parametric approaches such as simulated maximum likelihood (Mesters et al.; 2016). Especially for models of relatively high dimensions or with a rich dynamic structure, there is a lack of feasible estimation methods. Furthermore, in most empirical applications, methods are required to smoothly handle nonstationary cases alongside stationary ones.

We consider a computationally straightforward parametric treatment of fractional unobserved components models in state space form. An approximation of potentially non-

stationary fractionally integrated series using finite-order ARMA structures is suggested. This procedure outperforms the more commonly used truncation of fractional processes (cf. Chan and Palma; 1998) by providing a substantial reduction of the state dimension and hence of computational costs for a desired approximation quality. We derive both, the log likelihood and an analytical expression for the corresponding score. Hence, parameter estimation by means of the EM algorithm and gradient-based optimization make the approach feasible even for high dimensional datasets. In Monte Carlo simulations we study the performance of the proposed methods and quantify the accuracy of our state space approximation. For fractionally integrated and cointegrated processes of different dimensions, we find promising finite-sample estimation properties also in comparison to alternative techniques, namely the exact local Whittle estimator, narrow band least squares and exact state space methods. By using a parameter-driven state space approach, our setup inherits several additional favorable properties: Missing values are treated seamlessly, several types of structural time series components such as trends, seasons and noise can be added without effort, and a wide variety of possibly nonlinear or non-Gaussian observation schemes may be straightforwardly implemented; see Harvey (1991); Durbin and Koopman (2012).

In this paper we apply the proposed approximation scheme to a p -dimensional observed time series y_t , which is driven by a fractional components (FC) process as defined by Hartl and Weigand (2019),

$$y_t = \Lambda x_t + u_t, \quad t = 1, \dots, n. \quad (1)$$

Here, Λ is a $p \times s$ coefficient matrix with full column rank, the latent process $x_t = (x_{1t}, \dots, x_{st})'$ holds the purely fractional components which are driven by a noise process $\xi_t = (\xi_{1t}, \dots, \xi_{st})' \sim \text{NID}(0, I)$, and u_t holds the short memory components.

More precisely, while the stationary series u_t is only required to have a finite state space representation, the components of the s -dimensional x_t are fractionally integrated noise according to

$$\Delta^{d_j} x_{jt} = \xi_{jt}, \quad j = 1, \dots, s, \quad (2)$$

where for a generic scalar d , the fractional difference operator is defined by

$$\Delta^d = (1 - L)^d = \sum_{j=0}^{\infty} \pi_j(d) L^j, \quad \pi_0(d) = 1, \quad \pi_j(d) = \frac{j-1-d}{j} \pi_{j-1}(d), \quad j \geq 1, \quad (3)$$

and L denotes the lag or backshift operator, $Lx_t = x_{t-1}$. We adapt a nonstationary type II solution of these processes (Robinson; 2005) and hence treat $d_j \geq 0.5$ alongside the asymptotically stationary case $d_j < 0.5$ in a continuous setup.

The fractional unobserved components framework captures univariate and multivariate processes with both long-run and short-run dynamics, fractional cointegration and polynomial cointegration, as well as possibly high-dimensional processes with factor structure. It allows for an intuitive additive separation of long run and short run components, i.e. cyclical and trend components in business cycle analysis, while obtaining similar flexibility as (cointegrated) multivariate ARFIMA models. See Hartl and Weigand (2019) for the relation of the FC model to several other fractional integration setups.

The paper is organized as follows. Section 2 discusses the state space form, while section 3 outlines maximum likelihood estimation. In section 4, the estimation properties are investigated by means of Monte Carlo experiments before section 5 concludes.

2 The approximate state space form

2.1 Approximating nonstationary fractional integration

Unlike the stationary long-memory processes considered in the literature, e.g., by Chan and Palma (1998), Hsu et al. (1998), Hsu and Breidt (2003), Brockwell (2007), Mesters et al. (2016) as well as Grassi and de Magistris (2012), our nonstationary type II specification of fractional integration is straightforwardly represented in its exact state space form by setting starting values of the latent fractional process to zero, $x_{jt} = 0$ for $t \leq 0$. The solution for x_{jt} is based on the truncated operator $\Delta_+^{-d_j}$ (Johansen; 2008) and given by

$$x_{jt} = \Delta_+^{-d_j} \xi_{jt} = \sum_{i=0}^{t-1} \pi_i(-d_j) \xi_{j,t-i}, \quad j = 1, \dots, s.$$

For a given sample size n , x_t has an autoregressive structure with coefficient matrices $\Pi_j^d = \text{diag}(\pi_j(d_1), \dots, \pi_j(d_s))$, $j = 1, \dots, n$. Thus, a Markovian state vector embodying x_t has to include $n - 1$ lags of x_t and is initialized deterministically with $x_{-n+1} = \dots = x_0 = 0$. In principle, this exact state space form can be used to compute the Kalman filter, to evaluate the likelihood and to estimate the unknown model parameters by nonlinear optimization routines. Since the state vector is at least of dimension $s \cdot n$, this can become computationally very costly, particularly in large samples and for a large number s of fractional components, which makes a treatment of the system in its exact state space representation practically infeasible for a wide range of relevant applications.

For non-negative integration orders, note that the x_t can be generalized to have non-zero starting values x_0 . In that case, x_t is initialized via a diffuse initial state vector. Details on the initialization of nonstationary components are given in Koopman (1997).

Deterministic components in x_t are handled straightforwardly by defining $x_{jt}^* := x_{jt} + \mu_{jt}$ where $\text{Var}(\mu_{jt}) = 0 \forall j = 1, \dots, s$. Depending on the integration order d_j the contribution of μ_{jt} on y_t converges to a trend of degree $\lfloor d_j \rfloor$ as $t \rightarrow \infty$.

The literature on stationary long-memory processes has considered approximations based on a truncation of the autoregressive representation, considering only m lags of x_t for $m < n$ in the transition equation (i.e., setting all autoregressive coefficients to zero for $j > m$). Alternatively, the moving average representation has been truncated to arrive at a feasible state space model; see Palma (2007), sections 4.2 and 4.3.

Instead, we will apply ARMA approximations to the fractional state vectors, which provide a better approximation quality than the autoregressive or moving average truncation. An ARMA approximation of long-memory processes has been considered in the importance sampling frameworks of Hsu and Breidt (2003) and Mesters et al. (2016), but, arguably due to their computational burdens, did not find usage in applied research so far. In our setup, where fractional integration appears in the form of purely fractional components rather than ARFIMA processes, this approach is particularly convenient. In contrast to recent attempts to approximate ARFIMA processes by ARMA ones (discussed e.g. by Basak et al.; 2001), we do not freely estimate all ARMA parameters but only d , and thus retain the original parsimonious parameterization of the process.

As a (nonstationary) approximation of a generic univariate $x_t = \Delta_+^{-d} \xi_t$, we consider the process

$$\tilde{x}_t = \left[\frac{(1 + m_1 L + \dots + m_w L^w)}{(1 - a_1 L - \dots - a_v L^v)} \right]_+ \xi_t = \sum_{j=0}^{n-1} \tilde{\psi}_j(\varphi) \xi_{t-j}, \quad (4)$$

for finite v and w , where $\varphi := (a_1, \dots, a_v, m_1, \dots, m_w)'$ and all a_i and m_j are made functionally dependent on d to approximate x_t by \tilde{x}_t . In order to determine the parameters φ , we minimize the distance between x_t and \tilde{x}_t , using the mean squared error (MSE) over $t = 1, \dots, n$ as the distance measure. For given t , d and φ , we observe

$$\tilde{x}_t - x_t = \sum_{j=0}^{t-1} \tilde{\psi}_j(\varphi) \xi_{t-j} - \sum_{j=0}^{t-1} \psi_j(d) \xi_{t-j} = \sum_{j=0}^{t-1} (\tilde{\psi}_j(\varphi) - \psi_j(d)) \xi_{t-j}. \quad (5)$$

Hence, the MSE for period t is given by

$$E[(\tilde{x}_t - x_t)^2] = \text{Var}(\xi_t) \sum_{j=0}^{t-1} (\tilde{\psi}_j(\varphi) - \psi_j(d))^2,$$

while averaging over all periods for a given sample size n and ignoring the constant variance

term yields the objective function for a given d ,

$$\text{MSE}_n^d(\varphi) = \frac{1}{n} \sum_{t=1}^n \sum_{j=0}^{t-1} (\tilde{\psi}_j(\varphi) - \psi_j(d))^2 = \frac{1}{n} \sum_{j=1}^n (n-j+1) (\tilde{\psi}_j(\varphi) - \psi_j(d))^2. \quad (6)$$

The approximating ARMA coefficients are thus given by

$$\hat{\varphi}_n(d) = \arg \min_{\varphi} \text{MSE}_n^d(\varphi). \quad (7)$$

To obtain the approximating ARMA coefficients in practice, we conduct the optimization (7) over a reasonable range of d , such as $d \in [-0.5; 2]$, for a given n . Computational details of the optimization are given in Appendix A. Interestingly, for $d < 1$, stationary ARMA coefficients provide the minimum MSE, while for $d \geq 1$ we impose an appropriate number of unit roots to enhance the approximation quality.

To illustrate the results we plot the approximating ARMA(2,2) parameters as a function of d for $n = 500$; see figure 1. A closer look at the coefficients reveals that for $d > 0$ typically both the autoregressive and the moving average polynomial have roots close to unity which nearly cancel out. For example, to approximate a process with $d = 0.75$ we have $(1 - 1.932L + 0.932L^2)\tilde{x}_t = (1 - 1.285L + 0.306L^2)\xi_t$, which can be factorized as $(1 - 0.999L)(1 - 0.933L)\tilde{x}_t = (1 - 0.970L)(1 - 0.316L)\xi_t$. Despite their similarity, AR and MA roots do not cancel out for non-integer d , since the approximation quality is improved by additional free parameters. For integer integration orders the optimization yields $(1 - 0.953L)(1 - 0.477L)\tilde{x}_t = (1 - 0.953L)(1 - 0.477L)\xi_t$ for $d = 0$ and $(1 - L)(1 - 0.980L)\tilde{x}_t = (1 - 0.980L)(1 + 0.001L)\xi_t$ for $d = 1$. Consequently, our ARMA-approximation is consistent with the finite representation of inter-integrated processes.

To compare the ARMA(v, w) approximations with $v = w \in \{1, 2, 3, 4\}$ to a truncated AR(m) process, we contrast the approximating impulse response function $\tilde{\psi}_j$ to the true one, $\psi_j(d)$, for a given d . The autoregressive truncation lag $m = 50$ is used for our comparison, since this is among the largest values which we consider as feasible in a typical multivariate application. The result of this comparison is shown in figure 2 for $n = 500$ and $d = 0.75$. The autoregressive truncation approach gives the exact impulse responses for horizons $j \leq 50$, but then tapers off too fast. The ARMA approximations improves significantly over the autoregressive truncation whenever $v = w \geq 2$. For orders 3 or 4, the approximation error is even hardly visible. For the moving average truncation, the impulse responses equal zero for horizons exceeding the truncation lag (not shown).

To perform the comparison for different d , we plot the square root of the MSE (6) as a function of d for different approximation methods. For negative integration orders, as shown in figure 3, the moving average approach clearly outperforms the autoregres-

sion, while the ARMA method with orders $v = w > 2$ are better. The moving average approximation becomes inaccurate, however, for the case $d > 0$, and worse even than the autoregressive method as can be seen in figure 4. In contrast, the ARMA(3,3) and ARMA(4,4) approximations are well-suited to mimic fractional processes over the whole range of d . Further evidence in favor of the ARMA approximation will be presented in the Monte Carlo simulation of section 4.1.

2.2 The state space representations

Based on these methods we introduce the state space form of the multivariate model (1), where each x_{jt} is approximated by the ARMA approach. In the following we drop the tilde for the approximation of x_{jt} for notational convenience. To cover the very general case, we allow for residual auto- and cross-correlation by modelling the latent p -dimensional short memory process u_t via a stationary state space model, which can capture vector autoregressive, vector ARMA or factor models, among others, and include an additional noise term ε_t . The model can be written in state space form as

$$y_t = Z\alpha_t + \varepsilon_t, \quad \alpha_{t+1} = T\alpha_t + R\eta_t, \quad \eta_t \sim \text{NID}(0, Q), \quad \varepsilon_t \sim \text{NID}(0, H), \quad (8)$$

where the states may be partitioned into $\alpha_t' = (\alpha_t^{(1)'}, \alpha_t^{(2)'})$, the states related to the fractional and the stationary components, respectively.

Regarding the fractional part, we define $A_j^d := \text{diag}(\hat{a}_j(d_1), \dots, \hat{a}_j(d_s))$ and $M_j^d := \text{diag}(\hat{m}_j(d_1), \dots, \hat{m}_j(d_s))$ which contain the approximating AR and MA coefficients of the fractional noise introduced in section 2.1, while $A_j^d = 0$ for $j > v$ and $M_j^d = 0$ for $j > w$. Then $(I - A_1^d L - \dots - A_v^d L^v)(I + M_1^d L + \dots + M_w^d L^w)^{-1} \tilde{x}_t = \xi_t$. For a minimal state space representation, define $\mu_t := (I + M_1^d L + \dots + M_w^d L^w)^{-1} \tilde{x}_t$ such that $(I - A_1^d L - \dots - A_v^d L^v)\mu_t = \xi_t$. For $u = \max(v, w + 1)$, the first part of the state vector is a (us) -dimensional process $\alpha_t^{(1)'} = (\mu_t', \dots, \mu_{t-u+1}')$. Thus, $\alpha_{t+1}^{(1)} = T^{(1,1)}\alpha_t^{(1)} + R^{(1)}\eta_t^{(1)}$ with $\eta_t^{(1)} = \xi_t$, $R^{(1)'} = (I, 0, \dots, 0)'$, $Q^{(1,1)} = I$ and

$$T^{(1,1)} = \begin{bmatrix} A_1^d & A_2^d & \dots & A_u^d \\ I & & & 0 \\ \vdots & \ddots & & \vdots \\ 0 & \dots & I & 0 \end{bmatrix}.$$

The observation equation for the fractional part is $\tilde{x}_t = \mu_t + M_1^d \mu_{t-1} + \dots + M_{u-1}^d \mu_{t-u}$, which enters the observed process y_t through $A\tilde{x}_t = Z^{(1)}\alpha_t^{(1)}$. Thus, the observation matrix

for the fractional part is

$$Z^{(1)} = \begin{bmatrix} \Lambda & \Lambda M_1^d & \dots & \Lambda M_{u-1}^d \end{bmatrix}.$$

For the nonfractional part, we allow a general specification with $\alpha_{t+1}^{(2)} = T^{(2,2)}\alpha_t^{(2)} + R^{(2)}\eta_t^{(2)}$ and $u_t = Z^{(2)}\alpha_t^{(2)}$, where the distribution of unknown parameters over $T^{(2,2)}$ and $Z^{(2)}$ reflect the choice of the specific model. Without loss of generality, we set $Q^{(2,2)} = \text{Var}(\eta_t^{(2)}) = I$, so that scales and cross correlations of u_t are determined by $Z^{(2)}$. The full state space model (8) is given by an obvious definition of the system matrices as $Z = (Z^{(1)}, Z^{(2)})$, $R' = (R^{(1)'}, R^{(2)'})$, $T = \text{diag}(T^{(1,1)}, T^{(2,2)})$ and $Q = I$. The dynamics are complemented by the initial conditions for the states. From the definition of our type II fractional process we set fixed starting values such as $\alpha_0^{(1)} = 0$, while $\alpha_t^{(2)}$ is initialized by its stationary distribution.

The fractional components \tilde{x}_t do not explicitly appear as states in this representation. However, filtered and smoothed states can be constructed using the relation $\tilde{x}_t = \mu_t + \sum_{j=1}^w M_j^d \mu_{t-j}$. To obtain conditional covariance matrices for \tilde{x}_t , it is more convenient to use an alternative state space form of the ARMA process, where the MA coefficients appear in $R^{(1,1)}$ rather than in $Z^{(1)}$; see Durbin and Koopman (2012), section 3.4. The current setup, however, is appropriate for estimating the parameters via the EM algorithm which is discussed in the next section.

3 Maximum likelihood estimation

The EM algorithm was proposed for maximum likelihood estimation of state space models by Shumway and Stoffer (1982) and Watson and Engle (1983). Especially in the context of high-dimensional dynamic factor models with possibly more than hundred observable variables, i.e. $p > 100$, this method has been found very useful in finding maxima of high-dimensional likelihood functions; see, e.g., Quah and Sargent (1993), Doz et al. (2012) and Jungbacker and Koopman (2015). After rapidly locating an approximate optimum, the final steps until convergence are typically slow for the EM algorithm, and hence it has been suggested to switch to gradient-based methods with analytical expressions for the likelihood score at a certain step.

We will present these algorithms for our fractional model and thereby extend existing treatments in the literature. For the model represented by (8), the matrices T and Z both nonlinearly depend on d and other unknown parameters, so that there are nonlinear cross-equation restrictions linking the transition and the observation equation of the system.

The EM algorithm in general consists of two steps, which are repeated until con-

vergence. In the E-step the expected complete data likelihood is computed, where the expectation is evaluated for a given set of parameters $\theta_{\{j\}}$, while the M-step maximizes this function to arrive at the parameters used in the next E-step, $\theta_{\{j+1\}}$. Thus, we define $Q(\theta, \tilde{\theta}) := E_{\tilde{\theta}}[l(\theta)]$, where in this section all expectation operators are understood as conditional on the data y_1, \dots, y_n . In the course of the EM algorithm, after choosing suitable starting values $\theta_{\{1\}}$, the optimization $\theta_{\{j+1\}} = \arg \max_{\theta} Q(\theta, \theta_{\{j\}})$ is iterated for $j = 1, 2, \dots$ until convergence.

To state the algorithm for the model defined by (1) and specified further in section 2.2, we follow Wu et al. (1996) to obtain the expected complete data likelihood as

$$Q(\theta; \theta_{\{j\}}) = -\frac{n}{2} \log |Q| - \frac{1}{2} \text{tr} [RQ^{-1}R'(A_{\{j\}} - TB'_{\{j\}} - B_{\{j\}}T' + TC_{\{j\}}T')] \quad (9)$$

$$- \frac{n}{2} \log |H| - \frac{1}{2} \text{tr} [H^{-1}(D_{\{j\}} - ZE'_{\{j\}} - E_{\{j\}}Z' + ZF_{\{j\}}Z')],$$

where in our case $Q = I$, while T , Z and H are functions of the vector of unknown parameters θ and a possible dependence of the initial conditions for α_0 on θ has been discarded for simplicity. The conditional moment matrices $A_{\{j\}}$, $B_{\{j\}}$, \dots , are given in appendix B and can be computed by a single run of a state smoothing algorithm (Durbin and Koopman; 2012, section 4.4) based on the system determined by $\theta_{\{j\}}$.

Rather than carrying out the full maximization of $Q(\theta, \theta_{\{j\}})$ at each step, we obtain a computationally simpler modified algorithm. To this end, we partition the vector of unknown parameters as $\theta' = (\theta^{(1)'}, \theta^{(2)'})$ where $\theta^{(1)'} = (d', \lambda', \varphi')$, λ contains the unknown elements in A , φ holds the unobserved parameters for u_t in $T^{(2,2)}$ and $Z^{(2)}$, while the noise variance parameters in H are collected in $\theta^{(2)}$. First, the expectation / conditional maximization (ECM) algorithm described by Meng and Rubin (1993) in our setup amounts to a conditional optimization over $\theta^{(1)}$ for given variance parameters $\theta_{\{j\}}^{(2)}$ and optimization over $\theta^{(2)}$ for given $\theta_{\{j\}}^{(1)}$. Second, as suggested by Watson and Engle (1983), the optimization over $\theta^{(1)}$ is not finalized for each j , but rather a single Newton step is implemented for each iteration of the procedure. Neither of these departures from the basic EM algorithm hinders reasonable convergence properties.

A Newton step in the estimation of $\theta^{(1)}$ for given $\theta_{\{j\}}^{(2)}$ yields the estimate in the $(j+1)$ -th step

$$\theta_{\{j+1\}}^{(1)'} = (\Xi'_{\{j\}} G_{\{j\}} \Xi_{\{j\}})^{-1} \Xi'_{\{j\}} (g_{\{j\}} - G_{\{j\}} \xi_{\{j\}}). \quad (10)$$

The derivation of (10) and expressions for $\Xi_{\{j\}}$, $\xi_{\{j\}}$, $g_{\{j\}}$ and $G_{\{j\}}$ can be found in appendix B. Finally, the free variance parameters of H , collected in $\theta^{(2)}$, are estimated using the derivative of $Q(\theta, \theta_{\{j\}})$ with respect to H ; see (24). The estimate is given by the

corresponding elements of

$$\frac{1}{n}L_{\{j\}} := \frac{1}{n} \mathbb{E}_{\theta_{\{j\}}} \sum_{t=1}^n \varepsilon_t \varepsilon_t' = \frac{1}{n} (D_{\{j\}} - Z E_{\{j\}}' - E_{\{j\}} Z' + Z F_{\{j\}} Z').$$

For using gradient-based methods in later steps of the maximization, the likelihood score can be obtained with only one run of a state smoothing algorithm. This has been shown by Koopman and Shephard (1992), who draw on the result

$$\left. \frac{\partial Q(\theta, \theta_{\{j\}})}{\partial \theta} \right|_{\theta_{\{j\}}} = \left. \frac{\partial l(\theta)}{\partial \theta} \right|_{\theta_{\{j\}}},$$

where $l(\theta)$ denotes the Gaussian log-likelihood of the model. Evaluation of the score for our model can therefore be based on (22) and (24).

An estimate of the covariance matrix can be computed using an analytical expression for the information matrix. Denoting by v_t and F_t the model residuals and forecast error variances obtained from the Kalman filter, the i -th element of the gradient vector for observation t is given by

$$\frac{\partial l_t(\theta)}{\partial \theta_i} = -\frac{1}{2} \text{tr} \left[\left(F_t^{-1} \frac{\partial F_t}{\partial \theta_i} \right) (I - F_t^{-1} v_t v_t') \right] + \frac{\partial v_t'}{\partial \theta_i} F_t^{-1} v_t, \quad (11)$$

while the ij -th element of the information matrix $\mathcal{I}(\theta)$ is

$$\mathcal{I}_{ij}(\theta) = \frac{1}{2} \sum_{t=1}^n \text{tr} \left[F_t^{-1} \frac{\partial F_t}{\partial \theta_i} F_t^{-1} \frac{\partial F_t}{\partial \theta_j} \right] + \mathbb{E}_{\theta} \left[\sum_{t=1}^n \frac{\partial v_t'}{\partial \theta_i} F_t^{-1} \frac{\partial v_t}{\partial \theta_j} \right]; \quad (12)$$

see Harvey (1991, section 3.4.5). To obtain a feasible estimator $\hat{\mathcal{I}}(\hat{\theta})$, either the expectation term in (12) is omitted, as suggested by Harvey (1991), or the techniques of Cavanaugh and Shumway (1996) may be used to compute the exact Fisher information. An estimate of the covariance matrix of the estimator is then given by

$$\widehat{\text{Var}}_{\text{info}}(\hat{\theta}) = \hat{\mathcal{I}}(\hat{\theta})^{-1}, \quad (13)$$

or by the sandwich form

$$\widehat{\text{Var}}_{\text{sand}}(\hat{\theta}) = \hat{\mathcal{I}}(\hat{\theta})^{-1} \left[\sum_{t=1}^n \left. \frac{\partial l_t(\theta)}{\partial \theta} \right|_{\hat{\theta}} \left. \frac{\partial l_t(\theta)}{\partial \theta'} \right|_{\hat{\theta}} \right] \hat{\mathcal{I}}(\hat{\theta})^{-1}, \quad (14)$$

which is robust to certain violations of the model assumptions; see White (1982).

The asymptotic theory for maximum likelihood estimation in the fractionally coin-

tegrated state space setup with integration orders $d \in [0, 1.5)$ is derived in Hartl et al. (2020) for an exact representation of (2). As shown there, the approximation error of the Kalman filter that results from ARMA approximations can be calculated via (5) and is $E_\theta(\tilde{x}_t - x_t | y_1, \dots, y_{t-1})$. Hence, it is measurable given the σ -field generated by y_1, \dots, y_{t-1} , such that an approximation-corrected estimator can be constructed (Hartl et al.; 2020, Corollary 2.3). For this estimator, consistency and asymptotic (mixed) normality is shown. While the approximation-corrected maximum likelihood estimator is computationally feasible for long time series (i.e. n large), it is limited to low-dimensional y_t . Thus, especially for models where y_t typically holds a large number of observable variables, e.g. factor models, the proposed ARMA approximations provide a computationally feasible parametrization of state space models. We compare the performance of the maximum likelihood estimator for our approximate state space model with the approximation-corrected maximum likelihood estimator of Hartl et al. (2020) in a Monte Carlo study in section 4.1, where it will become clear that the mean squared error of the approximate estimator for d converges to the mean squared error of the exact estimator as n increases.

Our estimation approach can be straightforwardly generalized to additional situations of great practical relevance. To include a treatment of further components causing non-stationarity such as deterministic trends or exogenous regressors, one can use diffuse initialization of one or more of the states which may be based on Koopman (1997). While we have discussed maximum likelihood estimation under a setting where all data in y_t are available, our algorithms can be generalized for arbitrary patterns of missing data using the approach of Banbura and Modugno (2012). For very high-dimensional datasets, the computational refinements of Jungbacker and Koopman (2015) may be used. For common trends of similar persistence, nonparametric averaging methods may turn out to be useful (cf. e.g. Ergemen and Rodríguez-Caballero; 2016).

4 A Monte Carlo study

We study the performance of the described methods for a number of stylized processes which are nested in the general setup (1). The simulation study is designed to answer several questions. Firstly, we assess whether the finite-order ARMA approximation of the state space system performs well as compared to other parametric or semiparametric approaches. Secondly, we assess the feasibility of joint estimation of memory parameters and cointegration vectors in bivariate fractional systems with and without polynomial cointegration, again considering popular semiparametric approaches as benchmarks. Thirdly, the precision of cointegration estimators is studied in case of several cointegration relations of different strengths and for higher dimensions of the observed time series.

For each specification, we simulate $R = 1000$ replications and estimate the models using semiparametric estimates for d from the exact local Whittle estimator as starting values for maximum likelihood estimation. The coefficients of the unobserved components can be recovered via the variance of the fractionally differenced observables, since the disturbance terms are standardized. The precision of the estimators is assessed by the root mean squared error (RMSE) criterion or the bias or median errors of the parameter estimators, of state estimates or of out-of-sample forecasts. We vary over different sample sizes $n \in \{250, 500, 1000\}$ which cover relevant situations in macroeconomics and finance.

4.1 Finite state approximations in a univariate setup

As the simplest stylized setup of our model, we first assess the fractional integration plus noise case, which has been studied in a stationary setup, e.g., by Grassi and de Magistris (2012). For mutually independent ξ_t and ε_s , the data generating process is given by

$$\begin{aligned} y_t &= \Lambda x_t + \varepsilon_t, & t = 1, \dots, n, \\ \Delta^d x_t &= \xi_t, & \xi_t \sim NID(0, 1), \quad \varepsilon_t \sim NID(0, 1). \end{aligned} \tag{15}$$

The fractional integration plus noise model is a special case of (1) where $\Lambda = \sqrt{q}$, $u_t = \varepsilon_t$, $\text{Var}(\varepsilon_t) := h = 1$, and ξ_t, ε_t are independent. For the signal-to-noise ratio we consider $q \in \{0.5, 1, 2\}$, while the memory parameters $d \in \{0.25, 0.5, 0.75\}$ cover cases of asymptotically stationary and nonstationary fractional integration. We estimate the free parameters d, q and the noise variance h by maximum likelihood using the state space approach.

We apply different approximations to avoid an otherwise n -dimensional state process. Firstly, the ARMA(v, w) approximation given by (4) and (7) is considered, setting $v = w \in \{2, 3, 4\}$. The corresponding estimators are denoted as $\hat{d}_{v,w}$ in the result tables. Secondly, we assess truncations of the autoregressive representation of the fractional process at $m = 20$ and $m = 50$ lags as suggested in Palma (2007, section 4.2), and label these estimators \hat{d}_{AR20} and \hat{d}_{AR50} , respectively. Thirdly, moving average representations as proposed in Chan and Palma (1998) are used, also with a truncation at $m = 20$ and $m = 50$ lags (\hat{d}_{MA20} and \hat{d}_{MA50}). Furthermore, we employ the exact local Whittle (\hat{d}_{EW}) estimator of Shimotsu and Phillips (2005) as well as the univariate exact local Whittle approach (\hat{d}_{UEW}) as defined by Sun and Phillips (2004), which accounts for additive $I(0)$ perturbations. For both semiparametric estimators of the fractional integration order, we use $m = \lfloor n^{0.65} \rfloor$ Fourier frequencies as a common pragmatic choice. Using other typical values such as n^j , $j \in \{0.45, 0.5, 0.55\}$ would not change the results qualitatively, but $n^{0.65}$ is the best choice in most settings considered here. Finally, to grasp the performance of the exact maximum

likelihood estimator and to compare our approximate approach with it, we also include the approximation-corrected maximum likelihood estimator of Hartl et al. (2020), which corrects for the approximation error induced by ARMA(3,3) approximations.

The root mean squared errors of estimates of d for this setup are shown in table 1. Not surprisingly, for this stylized process with only three free parameters, the parametric approaches clearly outperform the semiparametric Whittle estimators. For the EW approach, the performance gets worse for more volatile noise processes (lower q), which is not the case for the UEW estimator. The bias of the EW estimator is negative due to the additive noise; see table 2 and also Sun and Phillips (2004). In contrast, the UEW estimator is positively biased, independently of q . Overall, it has inferior estimation properties, so that we do not show the UEW results for the other data generating processes.

Focusing on the state space approximations, we find that the ARMA approach for $v, w \geq 3$ is always among the best approaches. Overall, the ARMA(3,3) and ARMA(4,4) approximations exert a very similar performance, and their relative performance does not seem to depend on the specification of d and q . The truncation methods, in contrast, show mixed results. The moving average approximation tends to dominate the autoregressive one for smaller $d < 0.5$, which mirrors the conclusion from Grassi and de Magistris (2012) in their stationary setting. However, we find that the autoregression is better whenever nonstationary $d \geq 0.5$ or higher signal-to-noise ratios are considered.

As expected, the exact maximum likelihood estimator of Hartl et al. (2020) outperforms the approximation methods for most parameter settings. Considering the computational costs which are about 10 times higher than for the ARMA-approximations with $n = 250$, and about 250 times higher with $n = 1000$, the improvements are moderate, however. The median improvement in RMSE over the ARMA(3,3) across parameter setups is 7.7%. As the most extreme scenario, the RMSE can be reduced from 0.132 in the ARMA(3,3) method to 0.102 by the exact estimator for $n = 250$, $q = 0.5$, $d = 0.25$. As the signal-to-noise ratio q increases, benefits from the approximation-corrected estimator get smaller, and also an increase in the integration orders lowers the benefits from the approximation-corrected estimator. But most interestingly, the RMSE of the ARMA approximations converges to the RMSE of the approximation-corrected estimator as n increases. This indicates that for long time series, where the approximation-correction is particularly costly, it may not even be required.

Directing attention to table 2 again, we find that the bias for the ARMA approach for $v, w \geq 3$ does not contribute significantly to the estimation errors. Often, it does not appear until the third decimal place. The bias is generally small also for the truncation approaches, but there exist some situations where it is noticeable, mostly for larger d . There, larger sample sizes even tend to increase the bias, while higher truncation lags do

not always lessen the problem.

We investigate if the results carry over to estimation precision of the fractional components and to forecasting performance of the different approaches. This seems to be the case as table 3 shows. We restrict attention to the medium signal-to-noise case $q = 1$ and apply only the state space approaches. In the upper panel, the fractional component x_t is estimated by a Kalman smoother and the RMSE averages across all in-sample observations and iterations. We find rather small differences between the approaches, especially for small d , while ARMA(4,4) and ARMA(3,3) dominate the approximation-based methods in each constellation. The exact method is only slightly superior. The same holds for the forecasting performance, where 1- to 20-step ahead forecasts are evaluated against realized trajectories, again by their RMSE averaging both across horizons and iterations. The differences between the approaches are only slightly more pronounced than above, and again, ARMA(3,3) and ARMA(4,4) are very close to the best-performing exact method. Interestingly, with the low signal-to-noise ratio (not shown in the table), each approach does a poorer job to recover the underlying fractional component, and neither is able to appropriately separate the fractional from the noise component in any case.

In sum, we find good performance of the ARMA approximations. The ARMA(3,3) approach appears sufficient in typical empirical applications. This finding is very appreciable in light of the great reduction in computational effort: A fractional component is represented by 4 states, rather than by 50 in a truncation setup with inferior performance, while an approximation-corrected approach has higher computational costs especially for $n = 1000$ even in this very simple setup. Both these alternatives can easily become impractical in more complex situations.

Overall, the differences between the approximations account for a small fraction of the overall estimation uncertainty, even in this stylized setting with high overall estimation precision. Also the benefits of the approximation-corrected approach are limited. Together with the finding of accurate ARMA approximations in section (2.1), this suggests that the need of approximations might not be a serious obstacle to the state space modelling of fractional unobserved components.

4.2 A basic fractional cointegration setup

The performance of the state space approach in estimating fractionally cointegrated systems is studied in a bivariate process with short-run dynamics,

$$\begin{aligned} y_{1t} &= \Lambda_{11}x_t + \Gamma_{11}z_{1t}, & y_{2t} &= \Lambda_{21}x_t + \Gamma_{21}z_{1t} + \Gamma_{22}z_{2t}, \\ \Delta^d x_t &= \xi_t, & \xi_t &\sim NID(0, 1), \\ (1 - \phi_i L)z_{it} &= \zeta_{it}, & \zeta_{it} &\sim NID(0, 1), \quad i = 1, 2, \quad t = 1, \dots, n, \end{aligned} \quad (16)$$

with $\Lambda_{11} = \Lambda_{21} = 1$, $\Gamma_{11} = \Gamma_{22} = c$, $\Gamma_{21} = c \cdot e$, and $\phi_1 = \phi_2 = 0.5$. This implies that the true cointegration vector $B := \Lambda_{\perp} = (1, -1)'$, $B' \begin{pmatrix} y_{1t} & y_{2t} \end{pmatrix}' \sim I(0)$, where the first entry was normalized to one. Again the innovations are mutually independent. Note that $u_{1t} = cz_{1t}$, $u_{2t} = (c \cdot e)z_{1t} + cz_{2t}$, which allows for an interpretation of (16) as a fractionally cointegrated setup with cross- and autocorrelated short-run dynamics. We vary over values of the fractional integration order $d \in \{0.25, 0.5, 0.75\}$. The perturbation parameter $c \in \{0.5, 1, 2\}$ controls the signal-to-noise ratio and short-memory correlation between the processes is introduced, which will be governed by different values of $e \in \{0, 0.5, 1\}$. Cases where $\Gamma_{11} \neq \Gamma_{21}$ could be considered straightforwardly.

Here and henceforth, we apply the ARMA(3,3) approximation for maximum likelihood estimation of the unknown model parameters. In the current setup, the latter consist of the eight entries in $\theta' = (d, \phi_1, \phi_2, \Lambda_{11}, \Lambda_{21}, \Gamma_{11}, \Gamma_{21}, \Gamma_{22})$, where Γ_{ij} is the loading of z_{jt} on y_{it} , while the variance parameters are normalized to achieve identification. Starting values for the AR parameters are obtained by fitting an autoregressive model for the difference $y_{1t} - y_{2t}$. To contrast the properties to standard semiparametric approaches again, we apply the EW estimator componentwise to the univariate processes and investigate the mean of the univariate estimates. For the cointegration relation we apply the narrow-band least squares estimator which has been studied by Robinson and Marinucci (2001) in the nonstationary single equation case and by Hualde (2009) in a setup with cointegration subspaces (for details on cointegration subspaces, see Hualde and Robinson; 2010; Hartl and Weigand; 2019). We follow the literature which suggests to use a small number of frequencies and choose $\lfloor n^{0.3} \rfloor$, amounting to 5, 6 and 7 frequencies for our sample sizes.

Since the cointegration vectors are not identified without further restrictions, we investigate the angle ϑ between true and estimated cointegration spaces. Nielsen (2010) provides an expression for the sine of this angle, which is given in our framework by

$$\sin(\vartheta) = \frac{\text{tr}(\Lambda \hat{B})}{\|\Lambda\| \|\hat{B}\|}, \quad (17)$$

where \hat{B} is an estimated cointegration matrix and $\|A\|$ is the Euclidean norm of A . In the current bivariate setup with one cointegration relation, we have $\hat{B} = \hat{\Lambda}_\perp$ for the maximum likelihood estimator and $\hat{B}_{NB} = (1, -\hat{\beta}_{NB})'$ for the narrow-band least squares estimator $\hat{\beta}_{NB}$ applied to $y_{1t} = \beta y_{2t} + \text{error}$. Values of $\sin(\vartheta)$ closer to zero indicate preciser estimates and thus we compute the corresponding root mean squared error criterion as the square root of $\frac{1}{R} \sum_{i=1}^R \sin(\vartheta^i)^2$ in what follows. To get some intuition for the bivariate case, estimating a true value $B = (1, -1)'$ by $\hat{B} = (1, -1.1)'$ would result in a loss of $\sin(\vartheta) \approx 0.05$.

In table 4 we show root mean squared errors for memory parameters (\hat{d}^{ML} and \hat{d}^{EW}) and evaluate estimated cointegration spaces (by ϑ^{ML} and ϑ^{NB}) applying either the maximum likelihood or the semiparametric technique, respectively. Consider the case $e = 0$ first. Regarding the memory estimators, we find relatively large errors for this data generating process, with root mean squared errors frequently around 0.2 or larger, most prominently when the variances of the short-memory processes are large ($c = 2$). The Whittle estimator often performs better than maximum likelihood, especially for smaller c and d and in smaller samples.

For estimating the cointegration space, however, the state space approach appears worthwhile and outperforms narrow band least squares in most constellations. Not surprisingly, strong cointegration relations ($d = 0.75$) are precisely estimated, as is cointegration with small short-memory disturbances ($c = 0.5$). While the relative merits of maximum likelihood are unchanged for different cointegration strengths, we find that strong perturbations are better captured by the state space estimators. For $c = 2$, the RMSE of the semiparametric approach exceeds the parametric RMSE by about 70% in some cases.

Short memory correlation as introduced through $e > 0$ overall decreases the precision of the memory estimators. Interestingly, however, the performance of the cointegration estimators improves when $e > 0$ is considered. This is the case for both the maximum likelihood and the narrow band approach. To gain some insights into this finding, we assess the typical signed errors of the cointegration estimates. To this end, we consider a normalization of the cointegration vectors as $(1, -\beta)$, and assess estimated β for both approaches. Note that the narrow-band least squares estimator estimates β_{NB} directly, whereas β_{ML} is computed via $\beta_{ML} = -\hat{\Lambda}_{21}/\hat{\Lambda}_{11}$. For $\hat{\Lambda}_{11}$ small, the estimator becomes imprecise. Therefore, it is informative to compute an outlier-robust measure of the typical signed deviation. The median errors ($\text{median}_i(\hat{\beta}_j^i) - \beta_j$) for this data generating process are shown in table 5.

The typical deviations for the narrow band estimates exert a negative median bias of the estimates. A positive correlation between the short-memory components appears to work in the opposite direction so that the negative bias is reduced. In contrast, we find that the maximum likelihood estimators are essentially median-unbiased. Here, correlation

between the short-memory components may improve the distinction between short and long-memory components and hence reduce variability.

4.3 Correlated fractional shocks and polynomial cointegration

A further simulation setup extends the model setup (1) by introducing contemporaneously correlated $\xi_t \sim \text{NID}(0, S)$, and also allowing for polynomial cointegration through perfectly correlated ξ_t . Polynomial cointegration refers to a situation where lagged observations non-trivially enter a cointegration relation; see Granger and Lee (1989) as well as Johansen (2008, section 4) for nonfractional and fractional treatments, respectively. To motivate polynomial cointegration in terms of our model, assume for simplicity $d_1 > d_2 > \dots > d_s$. Let $\Lambda^{(1:(m-1))}$ hold the first $m - 1$ columns of Λ , and let $\Lambda_{\perp}^{(1:(m-1))}$ be its orthogonal complement. Then $\Lambda_{\perp}^{(1:(m-1))'} y_t \sim I(d_m)$ annihilates the first $m - 1$ common unobserved components $x_{1t}, \dots, x_{m-1,t}$. If a vector γ exists, such that $\gamma'(y_t' \Lambda_{\perp}^{(1:(m-1))}, \Delta^b y_{it})'$ is integrated of a lower order than d_m for any b and any $y_{it} \sim I(d_k)$, $k \in \{1, \dots, m - 1\}$, then polynomial cointegration occurs. Whenever $|\text{Cor}(\xi_{kt}, \xi_{mt})| = 1$, also x_{mt} and $\Delta^{d_k - d_m} x_{kt}$ are perfectly correlated, and hence there exists a linear combination $\gamma'(y_t' \Lambda_{\perp}^{(1:m)}, \Delta^{d_k - d_m} y_{it})'$ with a smaller integration order than d_m .

We consider

$$\begin{aligned} y_{1t} &= \Lambda_{11}x_{1t} + \Lambda_{12}x_{2t} + \varepsilon_{1t}, & y_{2t} &= \Lambda_{21}x_{1t} + \Lambda_{22}x_{2t} + \varepsilon_{2t}, & (18) \\ \Delta^{d_i} x_{it} &= \xi_{it}, & \xi_{it} &\sim \text{NID}(0, 1), & \text{Corr}(\xi_{1t}, \xi_{2t}) &= r, \\ \varepsilon_{it} &\sim \text{NID}(0, h_{ii}), & h_{ii} &= 1, & i &= 1, 2, \quad t = 1, \dots, n, \end{aligned}$$

where $\Lambda_{11} = \Lambda_{21} = 1$, $\Lambda_{12} = -\Lambda_{22} = a$, $d_1 > d_2$, and where we drop the assumption of orthogonal long-run shocks and allow for $\text{Var}(\xi_t) = Q \neq I$. Correlation between the innovations to the fractional processes is introduced through the parameter r . Besides the standard setting $r = 0$, we refrain from the assumption of independent components for $r = 0.5$, while $r = 1$ amounts to $\xi_{1t} = \xi_{2t}$ which is the case of polynomial cointegration since there is a second nontrivial cointegration relation in $(y_{1t}, y_{2t}, \Delta^{d_1 - d_2} y_{2t})'$. Combinations of $d_2 \in \{0.2, 0.4\}$ and $d_1 \in \{0.6, 0.8\}$ contrast relatively weak and strong cases of cointegration, while the importance of the component x_{2t} varies with $a \in \{0.5, 1, 2\}$. We treat $\theta = (d_1, d_2, \Lambda_{11}, \Lambda_{21}, \Lambda_{12}, \Lambda_{22}, r, h_{11}, h_{22})'$ as free parameters, but also investigate estimates imposing the singularity $r = 1$ when it is appropriate. Starting values for the fractional integration orders are obtained via the exact local Whittle estimator as in the preceding sections, where we consider the sum and the difference of y_{1t} and y_{2t} to estimate d_1 and d_2 . Initial values for r are obtained from the covariance of the fractionally

differenced processes $\text{Cov}(\Delta^{d_2}(y_{1t} - y_{2t}), \Delta^{d_1}(y_{1t} + y_{2t}))$.

Consider the results for $r = 0.5$ first. The root mean squared errors, shown in table 6, include estimators of cointegration spaces as above (evaluated by ϑ_1^{ML} and ϑ_1^{NB} in the table). Now, there are two memory parameters to be estimated either by maximum likelihood (\hat{d}_1^{ML} and \hat{d}_2^{ML}) or by the Whittle approach (\hat{d}_1^{EW} and \hat{d}_2^{EW}). Semiparametric estimates of d_2 are obtained from the narrow band least squares residuals. The table also contains the maximum likelihood estimate of the correlation parameter r (\hat{r}^{ML}).

For most parameter settings, we observe that the parametric memory estimators perform satisfactorily. They outperform the semiparametric approach whenever there is strong influence of the x_{2t} components ($a = 2$), most pronouncedly in larger samples. Also regarding cointegration estimators, higher values of a favor the parametric method. The correlation parameter is estimated with increasing precision in larger samples, while also the strength of the cointegration relation is relevant for this estimator. For $d_1 = d_2$, the correlation parameter (and also certain elements of Λ) would not be identifiable, and hence setups with small difference $d_1 - d_2$ are problematic.

For $r = 1$, we additionally consider the properties of estimators for the polynomial cointegration relation. To evaluate estimators of the polynomial cointegration spaces, note that the cointegration space leading to the highest memory reduction in $(y_{1t}, y_{2t}, \Delta^{d_1-d_2}y_{2t})'$ is the orthogonal complement of the span of

$$\begin{bmatrix} \Lambda^{(1)} & \Lambda^{(2)} \\ 0 & \Lambda_{21} \end{bmatrix}, \quad (19)$$

where $\Lambda^{(j)}$ refers to the j -th column of Λ . This cointegration subspace is estimated replacing all entries in (19) by their maximum likelihood estimates, where $r = 1$ is imposed. For the narrow band least squares estimator, this space is determined by the span of $(1, -\hat{\beta}_1, -\hat{\beta}_2)'$, where the coefficients are narrow band least squares estimates from $y_{1t} = \beta_1 y_{2t} + \beta_2 \Delta^{d_1-d_2} y_{2t} + \text{error}$ with d_1 and d_2 replaced by local Whittle estimates. Estimators for this second (polynomial) cointegration relation are evaluated analogously to (17) where now (19) takes the role of Λ and the resulting angle is denoted by θ_2 .

In table 7, the corresponding root mean squared errors are given. The elementary cointegration space is estimated by the unrestricted estimator (see ϑ_1^{ML}) and the restricted estimator (see ϑ_1^{RML} , imposing $r = 1$) with a very similar precision. This is in accordance with the notably precise estimation of r in this case. The parametric estimators of both cointegration spaces are again better than semiparametric approaches (1) in large samples and (2) when a strong second fractional component is present. Overall, the results suggest that polynomial fractional cointegration analysis is feasible in our setup, while the maxi-

mum likelihood approach has reasonable estimation properties at least for larger sample sizes.

4.4 Cointegration subspaces in higher dimensions

Until now, we have considered one- or two-dimensional processes in our simulations which limits the empirical relevance of the findings so far. We claim that modelling high-dimensional time series constitutes a strength of our approach, at least if suitably sparse parametrizations with factor structures are empirically reasonable. As a second generalisation compared to the previous setups, we consider situations where two or more cointegration relations exist and where these may be of different strength, i.e., where the reduction in memory through cointegration differs among relations. The latter situation has been studied under the label of cointegration subspaces, among others by Hualde and Robinson (2010) and Hartl and Weigand (2019).

To assess the performance in this situation, consider the process

$$\begin{aligned} y_{it} &= \Lambda_{i1}x_{1t} + \Lambda_{i2}x_{2t} + \varepsilon_{it}, \\ \Delta^{d_j}x_{jt} &= \xi_{jt}, \quad \xi_{jt} \sim NID(0, 1), \\ \varepsilon_{it} &\sim NID(0, h_{ii}), \quad h_{ii} = 1, \quad j = 1, 2, \quad i = 1, \dots, p, \quad t = 1, \dots, n, \end{aligned} \tag{20}$$

where $\Lambda_{i1} = a$, $\Lambda_{i2} = a \cdot (-1)^{i+1} \forall i = 1, \dots, p$, and with mutually independent noise sequences. We now vary over the dimension $p \in \{3, 10, 50\}$, while again combinations of $d_1 \in \{0.2, 0.4\}$ and $d_2 \in \{0.6, 0.8\}$ are considered. The parameter $a \in \{0.5, 1, 2\}$ gives the relative importance of the fractional components and hence plays the role of a signal-to-noise ratio. We estimate d_j , Λ_{ij} , h_i for $j = 1, 2$ and $i = 1, \dots, p$ as free parameters. Starting values for d_1 and d_2 are obtained as in section 4.3.

Along with the memory estimates, we show results for estimating the $p - 1$ cointegration relations reducing the memory from d_1 to d_2 (the first cointegration subspace) which is evaluated by the angle ϑ_1 between $\Lambda^{(1)}$ and the cointegration matrix estimate \hat{B}_1 . Additionally, the $p - 2$ cointegration relations reducing the memory from d_1 to 0 (the second cointegration subspace) are evaluated by the angle ϑ_2 between Λ and \hat{B}_2 . The cointegration matrices are straightforwardly obtained for the maximum likelihood approach by the orthogonal complements of $\hat{\Lambda}^{(1)}$ and $\hat{\Lambda}$, respectively. The narrow-band least squares method estimates cointegration matrices under specific normalizations as above. Estimating the first subspace, we construct \hat{B}_1 to have free entries $-\hat{\beta}_2, \dots, -\hat{\beta}_p$ in the first row and a $p - 1$ identity matrix below, such that β_j is obtained from $y_{jt} = \beta_j y_{1t} + \text{error}$ for $j = 2, \dots, p$. In the estimation of the second subspace, we have two free rows in \hat{B}_2 which

are given by $(-\hat{\beta}_{13}, \dots, -\hat{\beta}_{1p})$, and $(-\hat{\beta}_{23}, \dots, -\hat{\beta}_{2p})$, respectively, and can be estimated from $y_{jt} = \beta_{1j}y_{1t} + \beta_{2j}y_{2t} + \text{error}$ for $j = 3, \dots, p$.

In table 8, results are shown for $a = 0.5$ while the other specifications yield qualitatively similar outcomes. The process allows for a precise estimation of both d_1 and d_2 by maximum likelihood. An increasing dimension p leads to a better estimation by maximum likelihood which is not the case for the Whittle technique. The semiparametric Whittle estimates are obtained by averaging univariate estimates for d_1 and using narrow band least squares residuals to estimate d_2 . Notably, the estimates of d_2 hardly improve with larger n , which can be explained by a specific shortcoming of the single equation approach: The univariate regression errors may each have integration orders of d_2 or lower. In our case, lower orders prevail for $y_{jt} = \beta_j y_{1t} + \text{error}$ with j odd, due to the special structure of A . Knowledge about this specific structure is not exploited by both methods, however, to keep the simulation scenario realistic.

Also regarding the estimation of the cointegration spaces, maximum likelihood is superior. Both parametric and semiparametric estimators have smaller errors for higher dimension, whereas this “blessing of dimensionality” is more pronounced for the state space approach. Generally, the ratio between the maximum likelihood RMSE and the semiparametric RMSE decreases for larger p .

Not surprisingly, the case with strongest basic cointegration (large difference $d_1 - d_2$, which implies a great reduction of persistence when x_1 is projected out) is the one with highest precision in estimating the first cointegration subspace. For estimating the second subspace, a slightly different logic applies, with a larger d_2 supporting the estimation. E.g., in the case $d_1 = 0.6$ and $d_2 = 0.4$ a higher precision is achieved than for $d_1 = 0.6$ and $d_2 = 0.2$. Overall, we find that our approach profits from imposing the factor structure which is not the case for the benchmark methods applied in this comparison.

5 Conclusion

We have proposed estimation methods for nonstationary unobserved components models which are computationally efficient and provide a good approximation performance. These may be relevant for a wide variety of applications in macroeconomics and finance, as Hartl and Weigand (2019) have illustrated. Further work is needed to assess the performance of the methods in different, possibly very high-dimensional, settings.

Acknowledgements

The research of this paper has partly been conducted while Roland Weigand was at the University of Regensburg and at the Institute for Employment Research (IAB) in Nuremberg. Very valuable comments by Rolf Tschernig, Enzo Weber, and two anonymous referees, are gratefully acknowledged. Tobias Hartl gratefully acknowledges support through the projects TS283/1-1 and WE4847/4-1 financed by the German Research Foundation (DFG).

References

- Banbura, M. and Modugno, M. (2012). Maximum likelihood estimation of factor models on datasets with arbitrary pattern of missing data, *Journal of Applied Econometrics* **29**(1): 133–160.
- Barndorff-Nielsen, O. E. and Schou, G. (1973). On the parametrization of autoregressive models by partial autocorrelations, *Journal of Multivariate Analysis* **3**(4): 408–419.
- Basak, G. K., Chan, N. H. and Palma, W. (2001). The approximation of long-memory processes by an ARMA model, *Journal of Forecasting* **20**(6): 367–389.
- Brockwell, A. E. (2007). Likelihood-based analysis of a class of generalized long-memory time series models, *Journal of Time Series Analysis* **28**(3): 386–407.
- Cavanaugh, J. E. and Shumway, R. H. (1996). On computing the expected Fisher information matrix for state-space model parameters, *Statistics & Probability Letters* **26**(4): 347–355.
- Chan, N. H. and Palma, W. (1998). State space modeling of long-memory processes, *The Annals of Statistics* **26**(2): 719–740.
- Chen, W. W. and Hurvich, C. M. (2006). Semiparametric estimation of fractional cointegrating subspaces, *The Annals of Statistics* **34**(6): 2939–2979.
- Doménech, R. and Gómez, V. (2006). Estimating potential output, core inflation, and the NAIRU as latent variables, *Journal of Business & Economic Statistics* **24**(3): 354–365.
- Doz, C., Giannone, D. and Reichlin, L. (2012). A quasi-maximum likelihood approach for large, approximate dynamic factor models, *The Review of Economics and Statistics* **94**(4): 1014–1024.
- Durbin, J. and Koopman, S. J. (2012). *Time Series Analysis by State Space Methods: Second Edition*, Oxford Statistical Science Series.
- Ergemen, Y. E. and Rodríguez-Caballero, C. V. (2016). A dynamic multi-level factor model with long-range dependence, *CREATES Research Papers 2016-23*, Department of Economics and Business Economics, Aarhus University.
URL: <https://ideas.repec.org/p/aah/create/2016-23.html>
- Granger, C. W. J. and Lee, T. H. (1989). Multicointegration, in G. F. Rhodes and T. B. Fomby (eds), *Advances in Econometrics: Cointegration, Spurious Regressions, and Unit Roots*, JAI Press.

- Grassi, S. and de Magistris, P. S. (2012). When long memory meets the Kalman filter: A comparative study, *Computational Statistics & Data Analysis* (in press).
- Hartl, T., Tschernig, R. and Weber, E. (2020). Fractional trends in unobserved components models, *Papers*, arXiv.org.
URL: <https://arxiv.org/pdf/2005.03988.pdf>
- Hartl, T. and Weigand, R. (2019). Multivariate fractional components analysis, *Papers*, arXiv.org.
URL: <https://EconPapers.repec.org/RePEc:arx:papers:1812.09149>
- Harvey, A. C. (1991). *Forecasting, Structural Time Series Models and the Kalman Filter*, Cambridge Books, Cambridge University Press.
- Hassler, U. and Wolters, J. (1995). Long memory in inflation rates: international evidence, *Journal of Business & Economic Statistics* **13**(1): 37–45.
- Hsu, N.-J. and Breidt, F. J. (2003). Bayesian analysis of fractionally integrated ARMA with additive noise, *Journal of Forecasting* **22**(6-7): 491–514.
- Hsu, N.-J., Ray, B. K. and Breidt, F. J. (1998). Bayesian estimation of common long-range dependent models, in B. Grigelionis, J. Kubilius, V. Paulauskas, V. Statulevicius and H. Pragarauskas (eds), *Probability Theory and Mathematical Statistics: Proceedings of the Seventh Vilnius Conference*, VSP.
- Hualde, J. (2009). Consistent estimation of cointegrating subspaces. Universidad Pública de Navarra. Preprint.
- Hualde, J. and Robinson, P. (2010). Semiparametric inference in multivariate fractionally cointegrated systems, *Journal of Econometrics* **157**(2): 492–511.
- Johansen, S. (2008). A representation theory for a class of vector autoregressive models for fractional processes, *Econometric Theory* **24**(3): 651–676.
- Jungbacker, B. and Koopman, S. J. (2015). Likelihood-based dynamic factor analysis for measurement and forecasting, *The Econometrics Journal* **18**(2): C1–C21.
- Klinger, S. and Weber, E. (2016). Decomposing Beveridge curve dynamics by correlated unobserved components, *Oxford Bulletin of Economics and Statistics* **78**(6): 877–894.
- Koopman, S. J. (1997). Exact initial Kalman filtering and smoothing for nonstationary time series models, *Journal of the American Statistical Association* **92**(440): 1630–1638.

- Koopman, S. J. and Shephard, N. (1992). Exact score for time series models in state space form, *Biometrika* **79**(4): 823–826.
- Luciani, M. and Veredas, D. (2015). Estimating and forecasting large panels of volatilities with approximate dynamic factor models, *Journal of Forecasting* **34**: 163–176.
- Meng, X.-l. and Rubin, D. B. (1993). Maximum likelihood estimation via the ECM algorithm: A general framework, *Biometrika* **80**(2): 267–278.
- Mesters, G., Koopman, S. J. and Ooms, M. (2016). Monte Carlo maximum likelihood estimation for generalized long-memory time series models, *Econometric Reviews* **35**(4): 659–687.
- Morana, C. (2004). Frequency domain principal components estimation of fractionally cointegrated processes, *Applied Economics Letters* **11**(13): 837–842.
- Morana, C. (2007). Multivariate modelling of long memory processes with common components, *Computational Statistics & Data Analysis* **52**(2): 919 – 934.
- Morley, J. C., Nelson, C. R. and Zivot, E. (2003). Why are the Beveridge-Nelson and unobserved-components decompositions of GDP so different?, *The Review of Economics and Statistics* **85**(2): 235–243.
- Nielsen, M. Ø. (2004). Efficient inference in multivariate fractionally integrated time series models, *Econometrics Journal* **7**(1): 63i₂¹97.
- Nielsen, M. Ø. (2010). Nonparametric cointegration analysis of fractional systems with unknown integration orders, *Journal of Econometrics* **155**(2): 170–187.
- Palma, W. (2007). *Long-Memory Time Series: Theory and Methods*, Wiley.
- Quah, D. and Sargent, T. J. (1993). A dynamic index model for large cross sections, in J. H. Stock and M. W. Watson (eds), *Business Cycles, Indicators and Forecasting*, University of Chicago Press.
- R Core Team (2020). *R: A Language and Environment for Statistical Computing*, R Foundation for Statistical Computing, Vienna, Austria.
URL: <http://www.R-project.org/>
- Ray, B. K. and Tsay, R. S. (2000). Long-range dependence in daily stock volatilities, *Journal of Business & Economic Statistics* **18**(2): 254–262.
- Robinson, P. (2005). The distance between rival nonstationary fractional processes, *Journal of Econometrics* **128**(2): 283i₂¹300.

- Robinson, P. M. and Hualde, J. (2003). Cointegration in fractional systems with unknown integration orders, *Econometrica* **71**(6): 1727–1766.
- Robinson, P. and Marinucci, D. (2001). Narrow-band analysis of nonstationary processes, *Annals of Statistics* **29**(4): 947–986.
- Shimotsu, K. and Phillips, P. C. B. (2005). Exact local Whittle estimation of fractional integration, *The Annals of Statistics* **33**(4): 1890–1933.
- Shumway, R. H. and Stoffer, D. S. (1982). An approach to time series smoothing and forecasting using the EM algorithm, *Journal of Time Series Analysis* **3**(4): 253–264.
- Sun, Y. and Phillips, P. C. B. (2004). Understanding the Fisher equation, *Journal of Applied Econometrics* **19**(7): 869–886.
- Tschernig, R., Weber, E. and Weigand, R. (2013). Fractionally integrated VAR models with a fractional lag operator and deterministic trends: Finite sample identification and two-step estimation, *Regensburg Discussion Papers 471*, Universität $\frac{1}{2}$ t Regensburg.
- van Dijk, D., Franses, P. H. and Paap, R. (2002). A nonlinear long memory model, with an application to us unemployment, *Journal of Econometrics* **110**(2): 135 – 165. Long memory and nonlinear time series.
- Veenstra, J. Q. (2012). *Persistence and Anti-persistence: Theory and Software*, PhD thesis, Western University.
- Watson, M. W. and Engle, R. F. (1983). Alternative algorithms for the estimation of dynamic factor, MIMIC and varying coefficient regression models, *Journal of Econometrics* **23**(3): 385–400.
- White, H. (1982). Maximum likelihood estimation of misspecified models, *Econometrica* **50**(1): 1–26.
- Wu, L. S.-Y., Pai, J. S. and Hosking, J. (1996). An algorithm for estimating parameters of state-space models, *Statistics & Probability Letters* **28**(2): 99 – 106.

A Computational details of the approximating ARMA coefficients

As shown in (7) the ARMA approximation of a fractionally integrated process for a given integration order d is defined as the set of ARMA parameters that minimize (6). The minimization problem has a unique solution for $p+q \leq n$. We conduct the optimization (7) to obtain ARMA approximations of a fractional process over an appropriate, possibly nonstationary, range of d . For $d < 1$, we impose stability of the autoregressive polynomial, while imposing unit roots is found to enhance the numeric stability of the optimization for $d \geq 1$. In order to achieve numerically well-behaved optimizations, we work with transformed parameters and then re-transform them when the optimum is reached. First, the stable autoregressive and moving average parts are individually mapped to the space of partial autocorrelations so that they take values in $(-1, 1)$; see Barndorff-Nielsen and Schou (1973) and Veenstra (2012). Then, we apply Fishers z-transform $z = 0.5[\log(1+x) - \log(1-x)]$ to obtain an unconstrained optimization problem. For a given sample size n , we carry out an optimization for each value on a grid for d . We smooth the values using cubic regression splines before the result is re-transformed to the space of ARMA coefficients. In this way, we obtain a continuous and differentiable function $\hat{\varphi}_n(d)$. Whenever discontinuities occur in the space of transformed parameters (as for $d = 1$), we enforce a smooth transition between segments of $\hat{\varphi}_n(d)$ by the sine function. All computations in this paper are conducted using R (R Core Team; 2020).

B Details on the EM Algorithm

In this appendix, all necessary expressions for the computation of the EM algorithm will be given. The log-likelihood where the unobserved state process α_t is assumed known is called the complete data log likelihood and given by

$$l(\theta; \{y_t, \alpha_t\}_{t=1}^n) = -\frac{n}{2} \log |Q| - \frac{1}{2} \text{tr} \left[RQ^{-1}R' \sum_{t=2}^n (\alpha_t - T\alpha_{t-1})(\alpha_t - T\alpha_{t-1})' \right] \\ - \frac{n}{2} \log |H| - \frac{1}{2} \text{tr} \left[H^{-1} \sum_{t=1}^n (y_t - Z\alpha_t)(y_t - Z\alpha_t)' \right].$$

The expectation of the complete data likelihood, with expectation evaluated at parameters $\theta_{\{j\}}$, is denoted by $Q(\theta, \theta_{\{j\}})$ and given by (9). The terms involving expectations of the

(partially unobserved) data and its cross-moments are

$$\begin{aligned}
A_{\{j\}} &:= E_{\theta_{\{j\}}} \left[\sum_{t=2}^n \alpha_t \alpha_t' \right] = \sum_{t=2}^n \hat{\alpha}_t \hat{\alpha}_t' + \sum_{t=2}^n V_{t,t}, \\
B_{\{j\}} &:= E_{\theta_{\{j\}}} \left[\sum_{t=2}^n \alpha_t \alpha_{t-1}' \right] = \sum_{t=2}^n \hat{\alpha}_t \hat{\alpha}_{t-1}' + \sum_{t=2}^n V_{t,t-1}, \\
C_{\{j\}} &:= E_{\theta_{\{j\}}} \left[\sum_{t=2}^n \alpha_{t-1} \alpha_{t-1}' \right] = \sum_{t=2}^n \hat{\alpha}_{t-1} \hat{\alpha}_{t-1}' + \sum_{t=2}^n V_{t-1,t-1}, \\
D_{\{j\}} &:= E_{\theta_{\{j\}}} \left[\sum_{t=1}^n y_t y_t' \right] = \sum_{t=1}^n y_t y_t', \quad E_{\{j\}} := E_{\theta_{\{j\}}} \left[\sum_{t=1}^n y_t \alpha_t' \right] = \sum_{t=1}^n y_t \hat{\alpha}_t', \\
F_{\{j\}} &:= E_{\theta_{\{j\}}} \left[\sum_{t=1}^n \alpha_t \alpha_t' \right] = \sum_{t=1}^n \hat{\alpha}_t \hat{\alpha}_t' + \sum_{t=1}^n V_{t,t}.
\end{aligned}$$

Here, $\hat{\alpha}_t = E_{\theta_{\{j\}}}[\alpha_t]$ and $V_{t,s} = E_{\theta_{\{j\}}}[(\alpha_t - \hat{\alpha}_t)(\alpha_s - \hat{\alpha}_s)']$ can be computed by state smoothing algorithms based on the state space representation for given $\theta_{\{j\}}$ (Durbin and Koopman; 2012, section 4.4).

We turn to the derivation of (10). For notational convenience we denote the objective function for optimization over $\theta^{(1)}$ by $Q_{\{j\}}^{(1)}(\theta^{(1)}) \equiv Q((\theta^{(1)'}, \theta_{\{j\}}^{(2)'})'; \theta_{\{j\}})$. To describe the Newton step in the optimization of $Q_{\{j\}}^{(1)}$ in detail, we explicitly state the nonlinear dependence of $\text{vec}(T, Z)' = (\text{vec}(T)', \text{vec}(Z)')$ on $\theta^{(1)}$ by $\text{vec}(T, Z) = f(\theta^{(1)})$ and consider the linearization at $\theta_{\{j\}}$,

$$\text{vec}(T, Z) \approx \Xi_{\{j\}} \theta^{(1)} + \xi_{\{j\}}, \quad \text{where} \quad \Xi \equiv \frac{\partial f(\theta^{(1)})}{\partial \theta^{(1)'}}, \quad (21)$$

$\xi \equiv f(\theta^{(1)}) - \Xi \theta^{(1)}$, and the $\{j\}$ subscript indicates evaluation of a specific expression at $\theta_{\{j\}}$. The optimization over $\theta^{(1)}$ jointly involves elements in T and Z , since d enters the expression of both system matrices and hence, Ξ is not diagonal.

A single iteration of the Newton optimization algorithm is carried out by expanding the gradient around $\theta_{\{j\}}^{(1)}$. The gradient is given by

$$\frac{\partial Q_{\{j\}}^{(1)}(\theta^{(1)})}{\partial \theta^{(1)}} = \frac{\partial(\text{vec}(T)', \text{vec}(Z)')}{\partial \theta^{(1)}} \frac{\partial Q_{\{j\}}^{(1)}}{\partial(\text{vec}(T)', \text{vec}(Z)')} = \Xi' \text{vec} \left[\frac{\partial Q_{\{j\}}^{(1)}}{\partial T} \quad \frac{\partial Q_{\{j\}}^{(1)}}{\partial Z} \right], \quad (22)$$

where we drop the function argument of $Q_{\{j\}}^{(1)}(\theta^{(1)})$ for notational convenience. For the derivatives with respect to the system matrices we have

$$\frac{\partial Q_{\{j\}}^{(1)}}{\partial T} = (RQ^{-1}R')(B_{\{j\}} - TC_{\{j\}}) \quad \text{and} \quad \frac{\partial Q_{\{j\}}^{(1)}}{\partial Z} = H^{-1}(E_{\{j\}} - ZF_{\{j\}}),$$

so that

$$\text{vec} \begin{bmatrix} \frac{\partial Q_{\{j\}}^{(1)}}{\partial T} & \frac{\partial Q_{\{j\}}^{(1)}}{\partial Z} \end{bmatrix} = \begin{bmatrix} \text{vec}(RQ^{-1}R'B_{\{j\}}) \\ \text{vec}(H^{-1}E_{\{j\}}) \end{bmatrix} - \begin{bmatrix} C'_{\{j\}} \otimes RQ^{-1}R' & 0 \\ 0 & F'_{\{j\}} \otimes H^{-1} \end{bmatrix} \begin{bmatrix} \text{vec}(T) \\ \text{vec}(Z) \end{bmatrix}$$

Hence, for $G_{\{j\}}$ and $g_{\{j\}}$ given by

$$g_{\{j\}} = \text{vec}(RQ^{-1}R'B_{\{j\}}, H^{-1}E_{\{j\}}), \quad \text{and} \quad G_{\{j\}} = \text{diag}(C'_{\{j\}} \otimes RQ^{-1}R', F'_{\{j\}} \otimes H^{-1}),$$

we obtain the linear expansion

$$\frac{\partial Q_{\{j\}}^{(1)}(\theta^{(1)})}{\partial \theta^{(1)}} \approx \Xi'_{\{j\}} g_{\{j\}} - \Xi'_{\{j\}} G_{\{j\}} (\Xi_{\{j\}} \theta^{(1)} + \xi_{\{j\}}).$$

Equating to zero and solving for $\theta^{(1)}$ yields (10). For the estimation of H , see (24), we define

$$L_{\{j\}} := E_{\theta_{\{j\}}} \left[\sum_{t=1}^n \varepsilon_t \varepsilon_t' \right] = D_{\{j\}} - ZE'_{\{j\}} - E_{\{j\}}Z' + ZF_{\{j\}}Z'. \quad (23)$$

and use

$$\frac{\partial Q(\theta, \theta_{\{j\}})}{\partial H} = (H^{-1}L_{\{j\}} - nI)H^{-1} - 0.5 \text{diag}((H^{-1}L_{\{j\}} - nI)H^{-1}) \quad (24)$$

to derive the estimator of the variance parameters.

q	d	n	$\hat{d}_{2,2}$	$\hat{d}_{3,3}$	$\hat{d}_{4,4}$	\hat{d}_{AR20}	\hat{d}_{AR50}	\hat{d}_{MA20}	\hat{d}_{MA50}	\hat{d}_{EW}	\hat{d}_{UEW}	\hat{d}_{exact}
.5	.25	250	.130	.132	.132	.131	.130	.123	.122	.161	.414	.102
		500	.077	.075	.075	.075	.075	.075	.074	.138	.324	.069
		1000	.052	.050	.050	.051	.050	.051	.050	.119	.260	.048
	.50	250	.110	.109	.106	.122	.114	.106	.109	.191	.305	.089
		500	.068	.068	.068	.078	.071	.071	.070	.157	.212	.060
		1000	.045	.045	.044	.052	.047	.052	.048	.125	.140	.039
	.75	250	.098	.101	.100	.113	.100	.150	.125	.192	.223	.091
		500	.069	.066	.066	.096	.079	.108	.096	.148	.157	.066
		1000	.048	.044	.044	.086	.058	.084	.072	.108	.107	.046
1.0	.25	250	.086	.086	.086	.085	.085	.084	.083	.132	.413	.078
		500	.058	.057	.057	.057	.057	.057	.056	.111	.315	.053
		1000	.040	.038	.038	.039	.039	.039	.038	.090	.230	.037
	.50	250	.077	.078	.078	.086	.081	.082	.078	.145	.279	.072
		500	.056	.054	.054	.058	.057	.059	.057	.118	.188	.049
		1000	.038	.036	.036	.042	.038	.042	.040	.089	.125	.033
	.75	250	.076	.075	.075	.081	.075	.114	.096	.143	.200	.074
		500	.057	.054	.054	.066	.055	.086	.084	.111	.142	.054
		1000	.044	.037	.036	.068	.044	.059	.069	.079	.098	.038
2.0	.25	250	.072	.072	.072	.071	.072	.068	.068	.114	.402	.065
		500	.049	.048	.048	.048	.048	.047	.047	.094	.308	.044
		1000	.033	.032	.032	.033	.032	.033	.032	.072	.197	.031
	.50	250	.067	.066	.066	.075	.069	.071	.067	.118	.257	.062
		500	.049	.046	.046	.051	.049	.052	.050	.096	.178	.043
		1000	.034	.031	.031	.037	.034	.037	.035	.071	.117	.029
	.75	250	.067	.064	.064	.069	.065	.114	.088	.116	.187	.064
		500	.052	.046	.046	.057	.047	.108	.080	.093	.133	.046
		1000	.055	.032	.032	.060	.038	.098	.067	.066	.093	.033

Table 1: Root mean squared error (RMSE) for memory parameters in DGP1 (15). The columns show maximum likelihood estimators under ARMA(v,w) approximations of the fractional process with $v = w \in \{2, 3, 4\}$ ($\hat{d}_{v,w}$). Additionally, the truncated AR(m) representation (\hat{d}_{ARm}), and truncated MA(m) representations (\hat{d}_{MAm}) are given. Furthermore, we show the exact local Whittle (\hat{d}_{EW}) and the univariate exact local Whittle estimator (\hat{d}_{UEW}), each with $\lfloor n^{0.65} \rfloor$ Fourier frequencies. Finally, we include results for the approximation-corrected ML estimator (\hat{d}_{exact}).

q	d	n	$\hat{d}_{2,2}$	$\hat{d}_{3,3}$	$\hat{d}_{4,4}$	\hat{d}_{AR20}	\hat{d}_{AR50}	\hat{d}_{MA20}	\hat{d}_{MA50}	\hat{d}_{EW}	\hat{d}_{UEW}	\hat{d}_{exact}
.5	.25	250	-.019	-.019	-.019	-.027	-.025	-.032	-.032	-.125	.167	-.014
		500	-.012	-.010	-.010	-.012	-.015	-.015	-.018	-.112	.119	-.004
		1000	-.007	-.005	-.005	-.002	-.008	-.005	-.010	-.103	.094	.005
	.50	250	-.006	-.003	-.003	-.008	-.006	-.036	-.034	-.162	.095	-.010
		500	-.011	-.006	-.005	-.005	-.010	-.020	-.030	-.134	.040	-.008
		1000	-.012	-.003	-.003	.011	-.005	.002	-.017	-.110	.016	-.007
	.75	250	-.013	-.005	-.005	.012	-.003	-.052	-.066	-.163	.035	-.010
		500	-.016	-.007	-.006	.024	.002	-.036	-.067	-.123	.010	-.010
		1000	-.011	-.006	-.003	.046	.013	-.001	-.052	-.090	.004	-.010
1.0	.25	250	-.011	-.009	-.009	-.017	-.015	-.022	-.020	-.085	.207	-.009
		500	-.009	-.007	-.007	-.010	-.012	-.014	-.014	-.075	.139	-.004
		1000	-.006	-.004	-.003	-.002	-.006	-.005	-.008	-.067	.088	.003
	.50	250	-.006	-.002	-.002	-.005	-.004	-.036	-.028	-.104	.103	-.008
		500	-.009	-.005	-.004	-.005	-.007	-.024	-.027	-.084	.052	-.007
		1000	-.009	-.003	-.002	.008	-.003	-.005	-.016	-.067	.026	-.006
	.75	250	-.009	-.006	-.005	.009	-.003	-.068	-.068	-.101	.048	-.008
		500	-.005	-.008	-.006	.018	-.000	-.054	-.066	-.074	.023	-.009
		1000	.013	-.006	-.003	.039	.010	-.026	-.054	-.053	.015	-.008
2.0	.25	250	-.004	-.002	-.002	-.011	-.007	-.017	-.013	-.053	.224	-.006
		500	-.007	-.005	-.005	-.008	-.009	-.012	-.012	-.047	.148	-.004
		1000	-.004	-.002	-.002	-.001	-.004	-.005	-.006	-.041	.086	.002
	.50	250	-.001	.001	.001	.003	.001	-.033	-.020	-.061	.108	-.006
		500	-.004	-.003	-.003	-.001	-.003	-.026	-.023	-.049	.061	-.006
		1000	-.003	-.001	-.001	.008	-.000	-.010	-.015	-.038	.034	-.005
	.75	250	-.000	-.004	-.004	.009	-.002	-.068	-.067	-.059	.059	-.006
		500	.011	-.006	-.005	.017	-.000	-.055	-.066	-.043	.033	-.008
		1000	.041	-.003	-.003	.035	.009	-.030	-.055	-.030	.022	-.005

Table 2: Bias for memory parameters in DGP1 (15). The columns show maximum likelihood estimators under $ARMA(v,w)$ approximations of the fractional process with $v = w \in \{2, 3, 4\}$ ($\hat{d}_{v,w}$). Additionally, the truncated $AR(m)$ representation (\hat{d}_{ARm}), and truncated $MA(m)$ representations (\hat{d}_{MAm}) are given. Furthermore, we show the exact local Whittle (\hat{d}_{EW}) and the univariate exact local Whittle estimator (\hat{d}_{UEW}), each with $\lfloor n^{0.65} \rfloor$ Fourier frequencies. Finally, we include results for the approximation-corrected ML estimator (\hat{d}_{exact}).

d	n	$\hat{d}_{2,2}$	$\hat{d}_{3,3}$	$\hat{d}_{4,4}$	\hat{d}_{AR20}	\hat{d}_{AR50}	\hat{d}_{MA20}	\hat{d}_{MA50}	\hat{d}_{exact}
RMSE of estimated fractional component									
0.25	250	0.710	0.710	0.710	0.711	0.710	0.711	0.710	0.710
	500	0.708	0.708	0.708	0.708	0.708	0.708	0.708	0.707
	1000	0.707	0.707	0.707	0.707	0.707	0.707	0.707	0.707
0.50	250	0.700	0.700	0.700	0.701	0.700	0.704	0.701	0.699
	500	0.699	0.698	0.698	0.699	0.698	0.702	0.700	0.698
	1000	0.699	0.697	0.697	0.698	0.697	0.701	0.699	0.697
0.75	250	0.687	0.686	0.686	0.686	0.686	0.708	0.696	0.686
	500	0.687	0.685	0.685	0.685	0.685	0.709	0.697	0.685
	1000	0.687	0.684	0.684	0.685	0.684	0.713	0.699	0.684
RMSE of out-of-sample forecasts									
0.25	250	1.465	1.465	1.465	1.465	1.465	1.467	1.465	1.464
	500	1.463	1.463	1.463	1.464	1.463	1.465	1.464	1.463
	1000	1.438	1.438	1.437	1.439	1.437	1.440	1.438	1.438
0.50	250	1.680	1.678	1.678	1.688	1.681	1.733	1.697	1.677
	500	1.688	1.685	1.684	1.699	1.691	1.753	1.712	1.684
	1000	1.645	1.641	1.640	1.657	1.643	1.724	1.669	1.641
0.75	250	2.262	2.261	2.261	2.282	2.260	3.004	2.524	2.260
	500	2.290	2.287	2.285	2.353	2.309	3.227	2.707	2.286
	1000	2.201	2.191	2.191	2.264	2.212	3.394	2.677	2.191

Table 3: Upper panel: RMSE of estimating the fractional component x_t of DGP1 by the Kalman smoother. The RMSE averages across all in-sample observations and iterations. Lower panel: RMSE of forecasting a realized trajectory of DGP1 out-of-sample. The RMSE averages across all horizons from 1 to 20 and iterations.

c	d	n	e = 0				e = 0.5				e = 1			
			\hat{d}^{ML}	\hat{d}^{EW}	ϑ^{ML}	ϑ^{NB}	\hat{d}^{ML}	\hat{d}^{EW}	ϑ^{ML}	ϑ^{NB}	\hat{d}^{ML}	\hat{d}^{EW}	ϑ^{ML}	ϑ^{NB}
.5	.25	250	.204	.101	.212	.206	.255	.106	.216	.161	.277	.111	.219	.156
		500	.154	.087	.143	.161	.171	.091	.132	.122	.207	.095	.128	.120
		1000	.086	.075	.097	.125	.113	.079	.088	.097	.125	.086	.091	.098
	.50	250	.207	.122	.094	.082	.222	.126	.083	.066	.238	.134	.084	.063
		500	.126	.102	.052	.049	.143	.106	.045	.040	.151	.114	.042	.039
		1000	.086	.080	.025	.031	.094	.084	.021	.026	.097	.093	.022	.026
	.75	250	.188	.108	.042	.031	.192	.112	.030	.025	.203	.120	.022	.023
		500	.122	.089	.024	.017	.130	.092	.014	.014	.135	.099	.015	.013
		1000	.090	.067	.015	.009	.091	.069	.008	.008	.093	.075	.006	.008
1.0	.25	250	.266	.119	.358	.429	.309	.124	.365	.314	.344	.128	.374	.280
		500	.186	.124	.294	.367	.251	.128	.291	.262	.281	.133	.291	.238
		1000	.137	.126	.219	.315	.174	.130	.223	.231	.205	.137	.224	.216
	.50	250	.272	.195	.184	.195	.296	.202	.185	.153	.327	.216	.184	.148
		500	.169	.182	.098	.124	.192	.189	.092	.095	.217	.204	.098	.093
		1000	.102	.161	.060	.075	.114	.169	.051	.060	.124	.185	.051	.062
	.75	250	.210	.193	.056	.071	.231	.201	.052	.057	.238	.220	.050	.054
		500	.139	.161	.025	.037	.157	.169	.032	.030	.155	.188	.025	.028
		1000	.093	.127	.013	.019	.101	.134	.016	.017	.102	.151	.011	.016
2.0	.25	250	.306	.140	.519	.607	.343	.142	.509	.430	.396	.142	.516	.356
		500	.304	.161	.471	.572	.352	.163	.477	.396	.355	.164	.498	.330
		1000	.241	.174	.410	.539	.292	.176	.430	.380	.301	.179	.464	.325
	.50	250	.355	.297	.322	.413	.378	.302	.327	.302	.402	.309	.347	.271
		500	.277	.297	.207	.301	.306	.303	.213	.218	.338	.314	.234	.202
		1000	.175	.283	.117	.201	.191	.290	.120	.151	.219	.305	.125	.149
	.75	250	.261	.354	.106	.169	.294	.364	.102	.132	.317	.384	.112	.128
		500	.180	.317	.052	.088	.211	.328	.048	.069	.223	.350	.052	.066
		1000	.123	.270	.028	.043	.143	.281	.031	.036	.146	.305	.026	.036

Table 4: RMSE for parameters in DGP2 (16) for different specifications. The estimators arranged in columns are the ML estimator for d (\hat{d}^{ML}), the exact local Whittle estimator for d (\hat{d}^{EW}), the ML estimator for the cointegration space (ϑ^{ML}) and narrow band least squares for the cointegration space (ϑ^{NB}). The RMSE for cointegration spaces is based on the sine of the angle ϑ between the true and the estimated space (17).

c	d	n	$e = 0$				$e = 0.5$				$e = 1$			
			\hat{d}^{ML}	\hat{d}^{EW}	β^{ML}	β^{NB}	\hat{d}^{ML}	\hat{d}^{EW}	β^{ML}	β^{NB}	\hat{d}^{ML}	\hat{d}^{EW}	β^{ML}	β^{NB}
.5	.25	250	-.017	-.046	-.023	-.239	.006	-.047	-.038	-.179	.019	-.049	.000	-.198
		500	-.006	-.053	-.008	-.188	.012	-.057	-.012	-.146	.023	-.063	-.003	-.168
		1000	-.004	-.055	-.006	-.156	.010	-.058	-.011	-.123	.021	-.066	-.001	-.143
	.50	250	.027	-.069	.002	-.071	.035	-.073	.000	-.054	.032	-.083	.002	-.065
		500	.018	-.065	.004	-.041	.030	-.067	.002	-.031	.036	-.079	.001	-.037
		1000	.029	-.057	-.001	-.023	.043	-.060	.000	-.019	.042	-.071	.001	-.022
	.75	250	.046	-.061	.001	-.015	.046	-.066	.001	-.011	.043	-.076	.000	-.014
		500	.035	-.057	.002	-.006	.037	-.061	.001	-.006	.037	-.068	-.000	-.005
		1000	.059	-.045	.001	-.003	.057	-.047	.000	-.002	.053	-.055	.000	-.003
1.0	.25	250	-.035	-.092	-.102	-.556	-.016	-.091	-.052	-.383	-.006	-.089	-.041	-.377
		500	-.017	-.110	-.023	-.473	-.002	-.111	.012	-.344	-.002	-.116	.004	-.342
		1000	-.008	-.117	-.017	-.422	.002	-.121	-.007	-.308	.002	-.130	-.016	-.319
	.50	250	.014	-.173	-.006	-.213	.014	-.178	.002	-.166	.027	-.191	.000	-.185
		500	.007	-.166	.007	-.136	.007	-.172	.009	-.106	.012	-.187	.006	-.121
		1000	.013	-.151	-.002	-.083	.026	-.158	.000	-.067	.023	-.175	.001	-.078
	.75	250	.029	-.152	.000	-.051	.026	-.159	.002	-.039	.023	-.183	.001	-.047
		500	.022	-.135	.003	-.022	.024	-.140	.003	-.019	.017	-.160	-.000	-.022
		1000	.037	-.113	.000	-.010	.041	-.117	.000	-.008	.037	-.133	.000	-.010
2.0	.25	250	-.054	-.119	-.367	-.829	-.023	-.117	-.275	-.555	-.046	-.111	-.241	-.487
		500	-.037	-.148	-.156	-.766	-.014	-.148	-.144	-.536	-.059	-.148	-.278	-.470
		1000	-.020	-.167	-.077	-.731	-.005	-.169	-.084	-.517	-.037	-.172	-.253	-.470
	.50	250	-.043	-.286	-.053	-.525	-.048	-.285	-.028	-.369	-.047	-.290	-.008	-.358
		500	-.034	-.291	-.009	-.375	-.036	-.294	.004	-.276	-.023	-.307	.003	-.284
		1000	-.013	-.278	-.008	-.261	-.001	-.285	.005	-.205	.001	-.300	.004	-.215
	.75	250	-.033	-.347	-.007	-.168	-.041	-.354	-.001	-.127	-.020	-.372	.004	-.148
		500	-.035	-.310	.002	-.078	-.033	-.320	.002	-.062	-.021	-.339	.000	-.071
		1000	-.000	-.265	-.002	-.032	-.005	-.277	-.001	-.027	.001	-.299	.001	-.033

Table 5: Median errors for parameters in DGP2 (16) for different specifications. The estimators arranged in columns are the ML estimator for d (\hat{d}^{ML}), the exact local Whittle estimator for d (\hat{d}^{EW}), the ML estimator for the cointegration coefficient (β^{ML}) and narrow band least squares for the cointegration coefficient (β^{NB}).

a	d2	d1	n	\hat{d}_1^{ML}	\hat{d}_1^{EW}	\hat{d}_2^{ML}	\hat{d}_2^{EW}	ϑ_1^{ML}	ϑ_1^{NB}	\hat{r}^{ML}
.5	.2	.6	250	.154	.142	.306	.172	.260	.070	.121
			500	.176	.112	.310	.143	.326	.051	.090
			1000	.107	.081	.207	.126	.211	.038	.059
		.8	250	.148	.133	.268	.172	.177	.035	.059
			500	.165	.106	.264	.140	.215	.023	.034
			1000	.121	.079	.166	.123	.156	.014	.014
	.4	.6	250	.156	.137	.249	.214	.400	.122	.177
			500	.136	.108	.201	.178	.458	.102	.162
			1000	.109	.079	.167	.150	.461	.085	.145
		.8	250	.199	.131	.302	.214	.363	.064	.122
			500	.235	.105	.290	.176	.470	.048	.104
			1000	.279	.079	.306	.147	.581	.036	.075
2.0	.2	.6	250	.120	.247	.068	.119	.215	.361	.135
			500	.082	.216	.045	.089	.151	.222	.117
			1000	.058	.182	.030	.066	.093	.124	.062
		.8	250	.103	.248	.064	.113	.095	.137	.062
			500	.071	.200	.041	.086	.059	.074	.032
			1000	.052	.160	.028	.066	.033	.045	.011
	.4	.6	250	.122	.180	.068	.127	.435	.756	.224
			500	.084	.164	.048	.107	.369	.675	.213
			1000	.061	.147	.034	.085	.288	.551	.192
		.8	250	.110	.226	.067	.124	.214	.331	.172
			500	.076	.193	.045	.092	.153	.205	.149
			1000	.055	.164	.031	.069	.096	.129	.126

Table 6: RMSE for parameters in DGP3 (18) with $r = 0.5$. The estimators arranged in columns are the ML estimators for d_1 and d_2 (\hat{d}_1^{ML} and \hat{d}_2^{ML}), the EW estimator for d_1 and d_2 (\hat{d}_1^{EW} and \hat{d}_2^{EW}), the ML and NBLs estimators for the cointegration space $\mathcal{S}^{(1)}$ (ϑ_1^{ML} and ϑ_1^{NB}), as well as ML for r (\hat{r}^{ML}). The RMSE for cointegration spaces is based on the sine of the angle ϑ_j between the true and the estimated space (17).

a	d2	d1	n	\hat{d}_1^{ML}	\hat{d}_2^{ML}	ϑ_1^{ML}	ϑ_1^{RML}	ϑ_1^{NB}	ϑ_2^{RML}	ϑ_2^{NB}	\hat{r}^{ML}
.5	.2	.6	250	.149	.160	.170	.158	.095	.096	.093	.096
			500	.132	.139	.151	.085	.080	.054	.057	.054
			1000	.091	.082	.051	.042	.065	.029	.034	.029
		.8	250	.145	.134	.075	.047	.039	.033	.038	.033
			500	.099	.089	.048	.018	.028	.012	.018	.012
			1000	.067	.059	.032	.008	.019	.005	.009	.005
	.4	.6	250	.179	.259	.319	.324	.209	.148	.133	.148
			500	.157	.176	.329	.239	.196	.104	.099	.104
			1000	.176	.197	.573	.135	.180	.070	.072	.070
		.8	250	.184	.202	.251	.101	.092	.064	.049	.064
			500	.185	.202	.340	.050	.074	.034	.025	.034
			1000	.120	.121	.216	.023	.059	.016	.015	.016
2.0	.2	.6	250	.126	.079	.211	.205	.203	.064	.120	.064
			500	.090	.052	.126	.121	.206	.033	.073	.033
			1000	.062	.033	.064	.061	.196	.014	.029	.014
		.8	250	.095	.060	.056	.054	.094	.012	.040	.012
			500	.061	.042	.022	.020	.077	.003	.014	.003
			1000	.042	.030	.010	.010	.060	.002	.005	.002
	.4	.6	250	.128	.082	.379	.373	.820	.092	.276	.092
			500	.091	.057	.312	.290	.542	.068	.247	.068
			1000	.075	.040	.231	.213	.362	.044	.189	.044
		.8	250	.120	.067	.165	.161	.210	.050	.094	.050
			500	.077	.047	.080	.074	.204	.018	.040	.018
			1000	.049	.034	.031	.029	.183	.005	.014	.005

Table 7: RMSE for parameters in DGP3 (18) with $r = 1$. The estimators arranged in columns are the ML estimator for d_1 and d_2 (\hat{d}_1^{ML} and \hat{d}_2^{ML}), the restricted ML (setting $r = 1$), the ML and NBLs estimator for the cointegration space $\mathcal{S}^{(1)}$ (ϑ_1^{RML} , ϑ_1^{ML} and ϑ_1^{NB}), the restricted ML (setting $r = 1$) and NBLs estimator for the cointegration subspace $\mathcal{S}^{(2)}$ (ϑ_2^{RML} and ϑ_2^{NB}), as well as ML for r (\hat{r}^{ML}). The RMSE for cointegration spaces is based on the sine of the angle ϑ_j between the true and the estimated space (17).

d2	d1	p	n	\hat{d}_1^{ML}	\hat{d}_1^{EW}	\hat{d}_2^{ML}	\hat{d}_2^{EW}	ϑ_1^{ML}	ϑ_1^{NB}	ϑ_2^{ML}	ϑ_2^{NB}	
.2	.6	3	250	.125	.263	.108	.158	.074	.107	.037	.057	
			500	.087	.224	.078	.131	.046	.075	.020	.035	
			1000	.064	.187	.055	.115	.032	.048	.013	.023	
		10	250	.063	.268	.069	.157	.013	.029	.013	.036	
			500	.044	.226	.046	.129	.008	.019	.009	.033	
			1000	.029	.191	.030	.115	.006	.013	.006	.027	
	50	250	.054	.271	.059	.150	.002	.006	.002	.007		
		500	.037	.228	.039	.128	.001	.004	.001	.006		
		1000	.028	.189	.026	.113	.001	.002	.001	.005		
	.8	3	250	.104	.274	.108	.167	.033	.047	.018	.028	
				500	.077	.219	.076	.138	.020	.028	.009	.016
				1000	.059	.171	.053	.119	.013	.017	.005	.009
10			250	.064	.281	.070	.164	.007	.013	.012	.036	
			500	.045	.222	.047	.135	.004	.007	.009	.033	
			1000	.030	.175	.030	.120	.002	.004	.006	.027	
50		250	.055	.285	.059	.158	.001	.002	.002	.007		
		500	.037	.224	.039	.136	.001	.001	.001	.006		
		1000	.029	.173	.027	.118	.000	.001	.001	.005		
.4		.6	3	250	.121	.237	.121	.190	.163	.192	.034	.059
				500	.078	.204	.081	.150	.124	.159	.020	.035
				1000	.055	.173	.054	.125	.091	.129	.014	.024
	10		250	.062	.241	.065	.188	.028	.051	.011	.024	
			500	.044	.204	.045	.149	.017	.043	.008	.017	
			1000	.029	.175	.030	.124	.013	.035	.005	.011	
	50	250	.054	.243	.059	.184	.004	.010	.002	.004		
		500	.036	.207	.038	.148	.003	.008	.001	.003		
		1000	.028	.174	.027	.123	.002	.006	.001	.002		

Table 8: RMSE for parameters in DGP4 (20) with $a = 0.5$. The estimators arranged in columns are the ML estimator for d_1 and d_2 (\hat{d}_1^{ML} and \hat{d}_2^{ML}), the EW estimator for d_1 and d_2 (\hat{d}_1^{EW} and \hat{d}_2^{EW}), the ML and NBLs estimator for the cointegration space $\mathcal{S}^{(1)}$ (ϑ_1^{ML} and ϑ_1^{NB}), and the ML and NBLs estimator for the cointegration subspace $\mathcal{S}^{(2)}$ (ϑ_2^{ML} and ϑ_2^{NB}). The RMSE for cointegration spaces is based on the sine of the angle ϑ_j between the true and the estimated space (17).

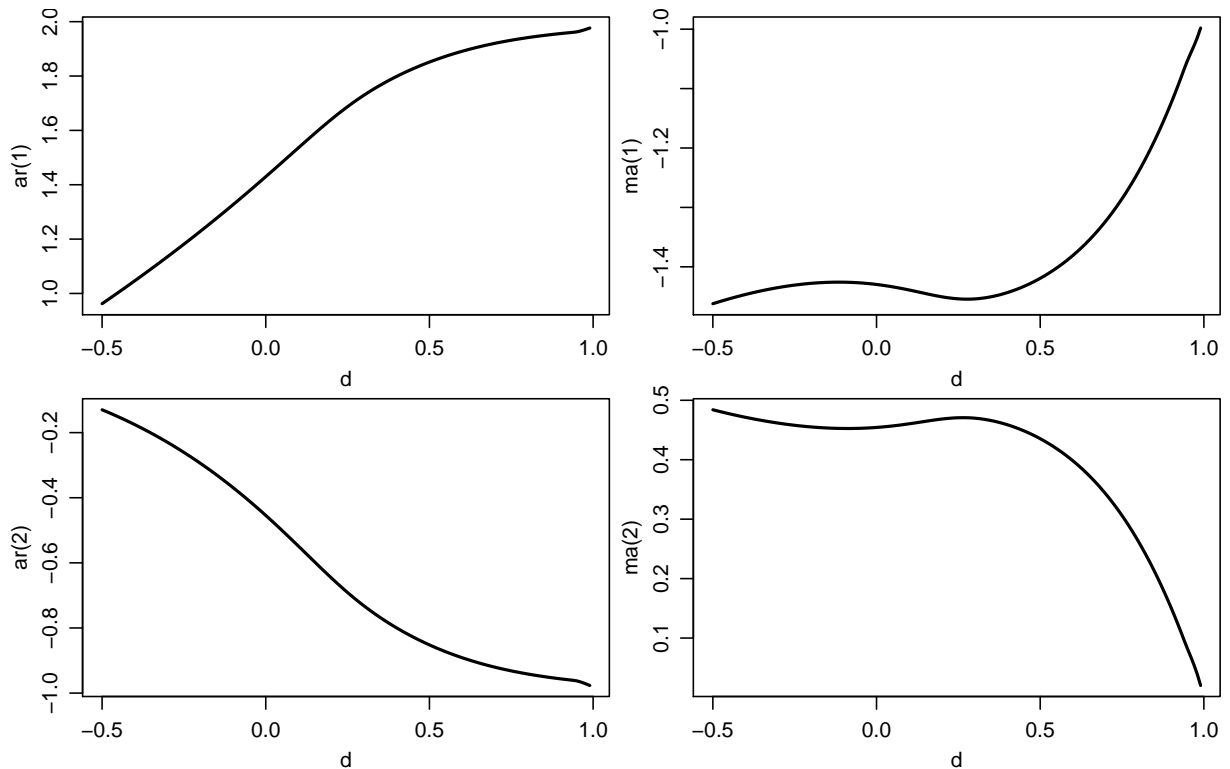


Figure 1: ARMA(2,2) coefficients (7) in the approximation of fractional processes for $d \in [-0.5; 1]$ and $n = 500$.

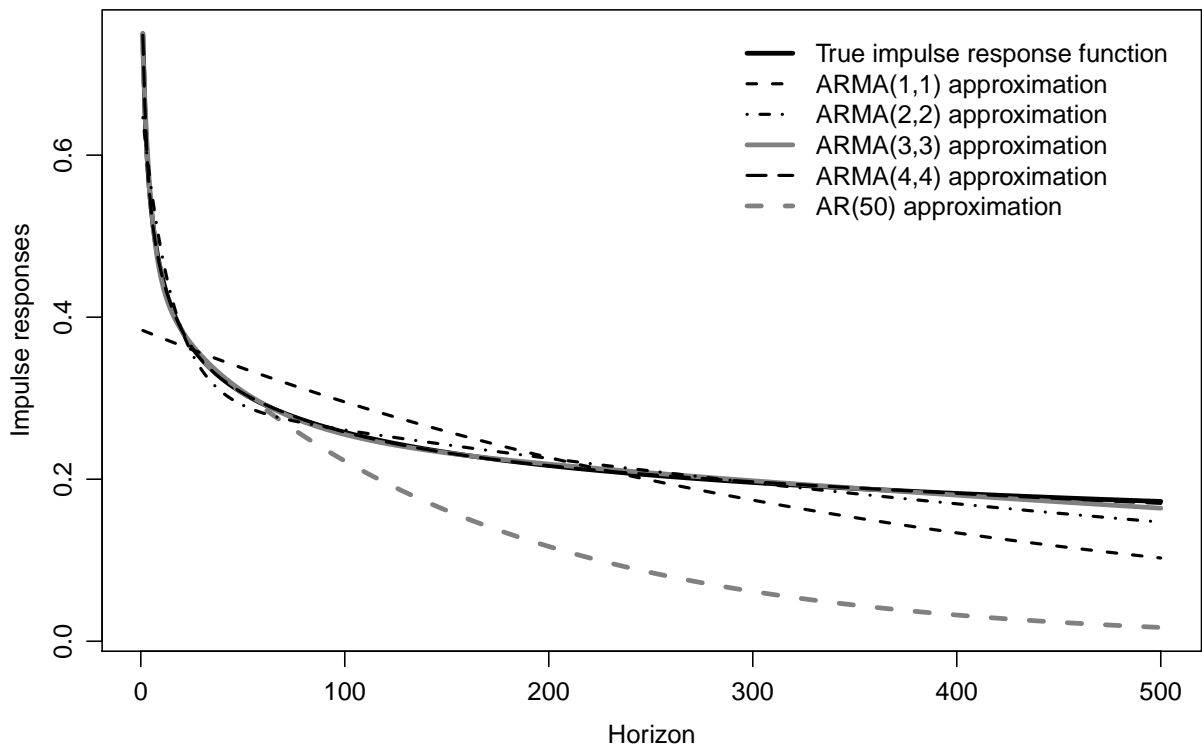


Figure 2: Impulse response functions $\tilde{\psi}_j$ (see (6)) for different approximating models for $d = 0.75$ and $n = 500$.

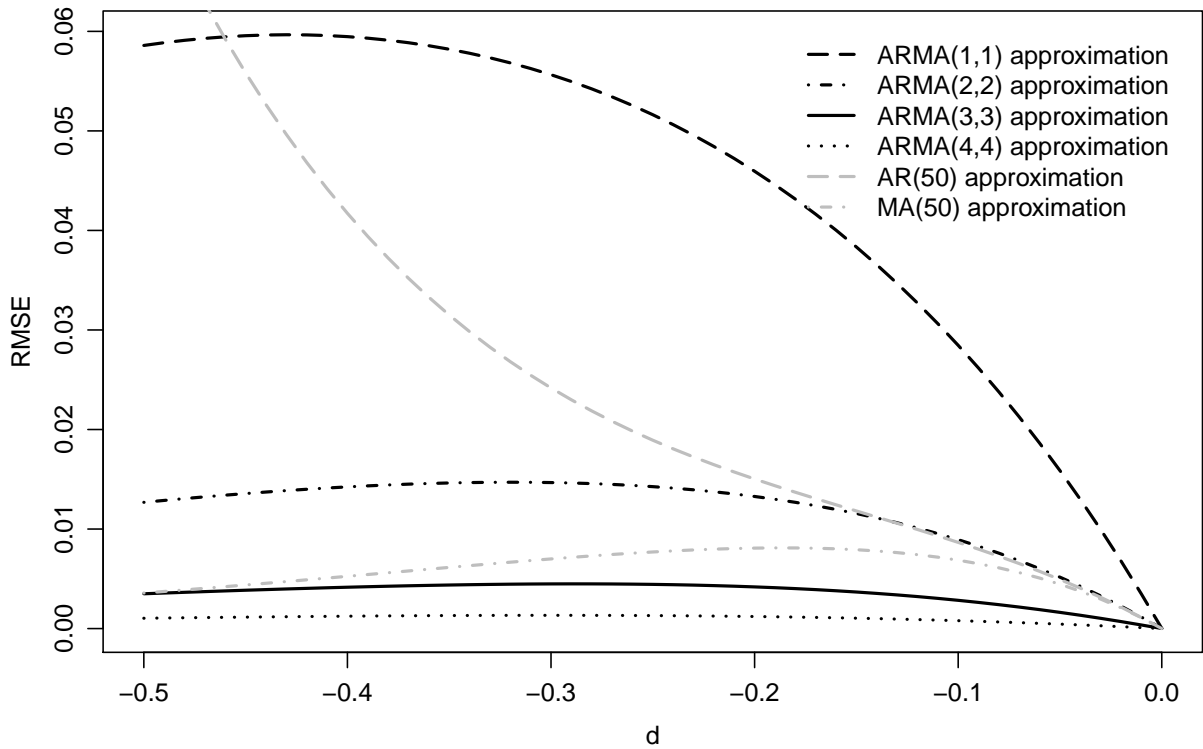


Figure 3: Root mean squared error (square root of (6)) for different approximating models, $d \in [-0.5; 0]$ and $n = 500$.

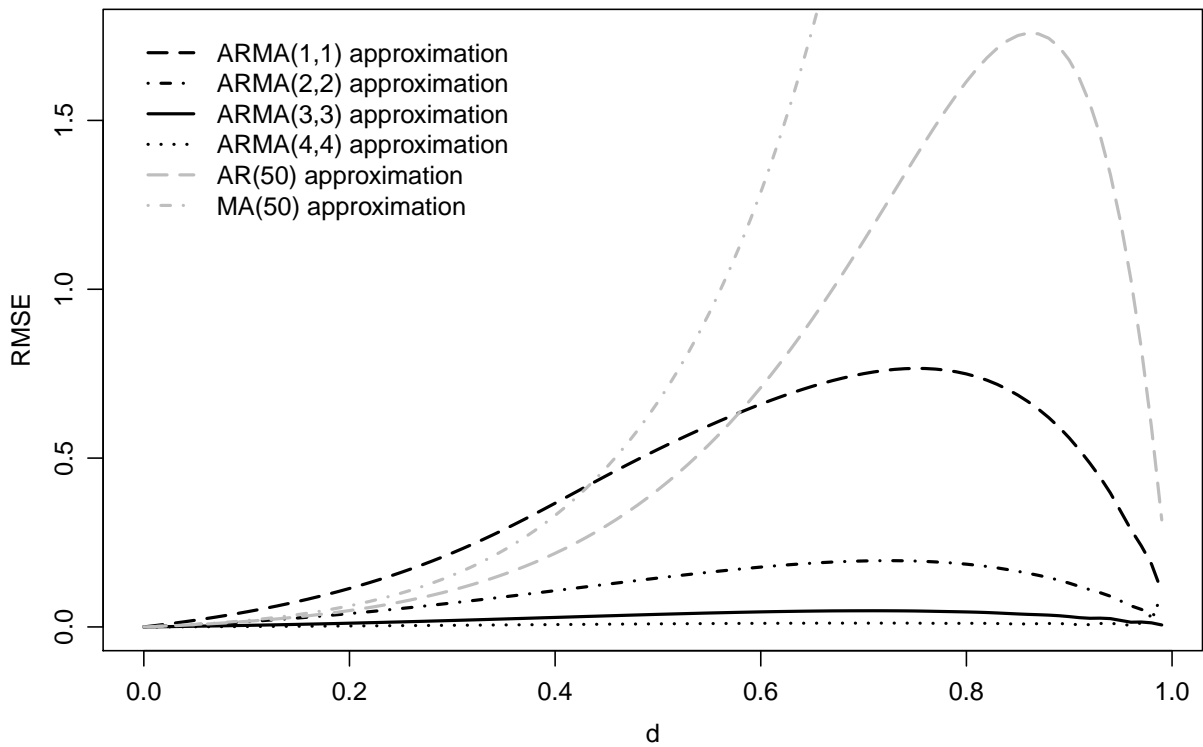


Figure 4: Root mean squared error (square root of (6)) for different approximating models, $d \in [0; 1]$ and $n = 500$.